Structure and function of the hybrid cluster protein

Hagen, Wilfred R.

DOI
10.1016/j.ccr.2021.214405

Publication date
2022

Document Version
Final published version

Published in
Coordination Chemistry Reviews

Coordination Chemistry Reviews 457 (2022) 214405

Contents lists available at ScienceDirect

Coordination Chemistry Reviews

journal homepage: www.elsevier.com/locate/ccr

Review

Structure and function of the hybrid cluster protein

Wilfred R. Hagen

Department of Biotechnology, Delft University of Technology, Building 58, Van der Maasweg 9, 2629HZ Delft, The Netherlands

ARTICLE INFO

Article history:
Received 5 June 2021
Received in revised form 8 November 2021
Accepted 30 December 2021

Keywords:
Hybrid cluster protein
Prismane protein
NO reductase
Persulfide
S-nitrosylase
CO dehydrogenase

ABSTRACT

A hybrid cluster (HC) is a 4Fe cluster with both sulfur and oxygen bridges. Hybrid cluster proteins (Hcps) contain two 4Fe clusters, a one electron transferring iron-sulfur cluster and a hybrid cluster. The structural gene, *hcp*, is diffusely found in bacteria, archaea, and monocellular eukarya, and the HC binding motif involving amino acids H, E, C, C, C, C, E, (K) appears to be fully conserved. HC is the active site of the enzyme Hcp. Of several reported Hcp enzymatic activities the conversion of nitric oxide into nitrous oxide, NO reductase, has been established as physiologically relevant. Other activities, notably signal transduction by NO transfer to other proteins, are controversial. The HC undergoes a complex structural change associated with single-electron iron based redox chemistry as well as electron-pair redox chemistry of a persulfidocysteine sulfur atom. A mechanistic scheme is proposed for the HC encompassing its structural, magnetic, and enzymatic properties.

Contents

E-mail address: w.r.hagen@tudelft.nl

https://doi.org/10.1016/j.ccr.2021.214405
0010-8545/

1. Introduction

The hybrid cluster protein (Hcp) was discovered serendipitously in 1988 in the bacterium *Desulfovibrio vulgaris* as a 60-kDa monomeric iron-sulfur protein of unknown function, and was originally named the prismane protein [1]. Follow-up studies came in three subsequent waves of research dominated respectively by magnetic spectroscopy, protein crystallography, and genetics-physiology, culminating today in a quest to link the full set of its structural elements to Hcp's molecular mechanism in biological functioning.

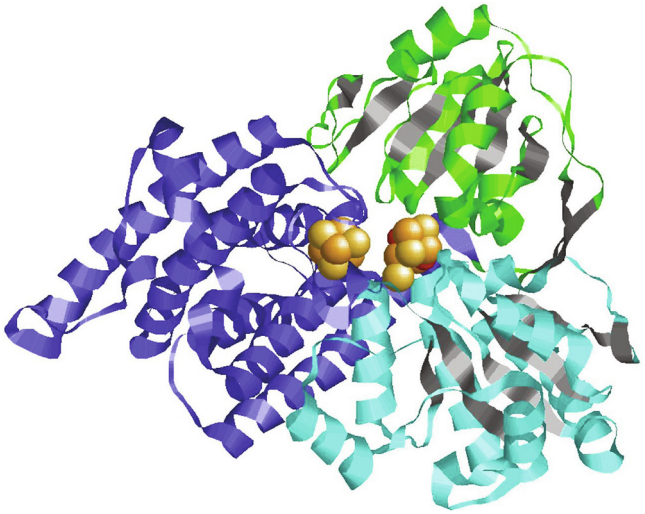

Fig. 1. The hybrid cluster protein consists of three domains. This picture is for *D. vulgaris* Hcp (1GNT.pdb). Domain 1 (dark blue) is predominantly α-helical and comprises two perpendicular bundles each consisting of three anti-parallel helices. The electron-transferring iron-sulfur cluster is bound near the N-terminus of domain 1. Domains 2 and 3 each consist of a central β-sheet (gray) with helices on either side (green for domain 2 and cyan for domain 3). The hybrid cluster is coordinated jointly by scattered residues of domains 2 and 3.

In a nutshell, Hcp contains two metal clusters each with four iron ions, one is a garden-variety [4Fe-4S]$^{(2+;1+)}$ electron-transfer cluster, the second one, the active site, is the hybrid cluster, an unprecedented structure in which irons are bridged by sulfur, μ_2-S^{2-} and μ_3-S^{2-} and by oxygen, μ_2-O^{2-} [2]. As illustrated in Fig. 1, the protein is made up of three domains: domain 1 is predominantly α-helix and binds the regular [4Fe-4S] cluster near the N-terminus of the protein. Domains 2 and 3 each consist of a central β-sheet with helices on either side, and together they bind the hybrid cluster, which is roughly located in the middle of the protein. The Hcp is a nitric oxide reductase [3], and it may also function in NO transfer to other proteins [4]. The structural gene *hcp* is widely, but not ubiquitously, distributed amongst the bacteria, archaea, and mono-cellular eukarya. In facultative anaerobes hcp is only expressed during oxygen-limited or anaerobic growth; the gene has not been found in obligatory aerobic bacteria. Furthermore, it does not appear to be present in higher eukarya, including man. Hcp is likely to be of medical interest as an important enzyme in human pathogens protecting against host NO attack. The *hcp* gene shows significant homology with the gene of only one other protein, the nickel–iron containing carbon monoxide dehydrogenase (COdh). The active-site clusters of both enzymes undergo drastic structural changes as a function of redox state [5,6].

For reference throughout the review these changes in Hcp are illustrated in Fig. 2. Fe and S counting starts at 5 because the numbers 1–4 are reserved for the cubane cluster. Numbering of bridging oxygens starts at 8 in a sequel to the sulfur numbering of 5–7. Briefly, when the irons in the fully reduced cluster (RED) release one (SEMI) or two (OX) electrons Fe8 moves over a distance of ca 2 Å, and three μ_2-O bridges are formed. Also, the μ_3-S bridge of S7 is broken and S7 moves over ca 4 Å to become η_1-S as part of a persulfidocysteine ligand to Fe8. A detailed discussion of these complex changes is deferred to Section 6 when the reader will be armed with background knowledge on redox chemistry and paramagnetism of the HC, on its protein binding motif, and on its putative substrates and activities.

This review covers the complete Hcp literature from 1989 till now. Previously only one other review has been published in 1999 [7] shortly after the first X-ray structure was determined

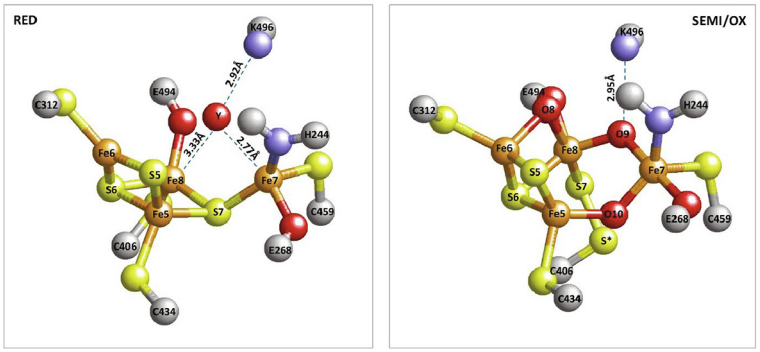

Fig. 2. Comparison of *D. vulgaris* hybrid cluster structures in RED versus OX/SEMI states. The figure was constructed from pdb files 1OA1 (RED) and 1W9M (SEMI). The cluster core in the RED state is [4Fe 2μ_3-S μ_2-S (O)] and in the OX/SEMI states it is [4Fe μ_3-S μ_2-S η_1-S* 3μ_2-O] These redox-dependent structural changes are addressed in detail in section 6.

[2], but before it became clear that the hybrid cluster can undergo extensive structural changes [5], and also preceding all functional studies [3,4,8,9].

2. Elemental biochemistry

2.1. Discovery of the hybrid cluster protein

In 1989 ohmics were still in their infancy with six more years to go until the first complete genome sequence ever was published, and therefore the only alternative to the classical approach of discovering 'novel' enzymes by following activity chromatographically at that time was visual inspection of chromatograms. Indeed in bioinorganic chemical research it was quite popular to load microbial cell-free extracts on separation columns and to look for coloured bands in the eluate as a sign of proteins containing transition metals with potentially interesting magneto-spectroscopic properties. Thus enters the Hcp as a brownish band partially overlapping with the band of FeFe-hydrogenase in cell-free extract of *Desulfovibrio vulgaris*, sub-strain Hildenborough [1]. Once purified the dithionite-reduced Hcp gave a single S = 1/2 signal in EPR with g values 2.004, 1.819, 1.32, which were unprecedented in metalloprotein EPR, but which closely matched the g values 2.029, 1.79, 1.3 of the $[6Fe\text{-}6S]^{3+}$ prismane core in the synthetic compound $(Et_4N)_3[Fe_6S_6(SC_6H_4\text{-}p\text{-}Me)_6]$ [10]. Combined with the elemental analysis of 6.3 Fe and 6.2 S per 52-kDa protein the conclusion was readily drawn that the protein was likely to contain a prismane-like cofactor, hence the name prismane protein.

In hindsight this erroneous assignment can be traced back to two unusual facts. First, for want of the sequence of the structural gene, sedimentation-equilibrium runs in an analytical ultracentrifuge were used as presumed most reliable method to determine molecular weight [11]. The result of 52 kDa later turned out to be off by 15% compared to the gene-predicted value of 60 kDa (therefore: 7.3 Fe and 7.2 S) presumably due to inaccuracy in the protein's partial specific volume value. Second, it became clear in the course of time that the EPR spectrum contained a second signal [12,13], which was initially overlooked due to its extreme width and therefore low intensity, and which eventually could be assigned to the [4Fe-4S] cluster [14]. Initially, however, the proposal of a prismane-like cluster was found to be so convincing that Mössbauer spectroscopic results were interpreted to be fully consistent with a single 6Fe cluster [15] or even with two different 6Fe clusters [12]. A crystallographic protein structure determination was required to eventually transfer the concept of a biological prismane-like cluster to the realm of fables [2].

2.2. Nomenclature

The name prismane has remained to be associated with the Hcp up to this day, for example in annotations, by sequence homology, of genomes. In the PFAM (protein families) database the designation 'prismane' is used in its listings of architectures, or domain organizations, to identify the binding pattern of the hybrid cluster (pfam.xfam.org/family/Prismane). Even after the hybrid cluster had been given its name in the first Hcp crystallographic structure paper, the habit of identifying the Hcp as prismane protein lingered on for some time. Alternative names were also proposed, e.g., 'Fepr' in the 1999 review on Hcp [7], or 'fuscoredoxin' (brownish redox protein) in the work of the Moura's [16,17]. We preferred to extend the name 'hybrid cluster' to also be part of the name of the protein as 'hybrid cluster protein' [18] and this has become general practice now.

After I determined, with analytical chemistry, that the active site of FeFe-hydrogenase contains 6 Fe [19] and, using EPR spectroscopy, that the P-cluster in nitrogenase contains 8 Fe [20], I proposed in 1992 that these enzymes together with the presumed 6 Fe-cluster containing prismane protein, and the enzyme CO dehydrogenase (whose unusual paramagnetism [21,22] exhibits similarity to that of the prismane protein [15]) all should be classified as Fe-S proteins containing 'superclusters', or Fe-S clusters with more than 4 Fe and exhibiting multiple redox transitions [15,23]. The underlying idea was of course to probe these enzymes for common spectroscopic, structural, and mechanistic properties. The name 'superclusters' has not stood the test of time, but a similar name in a similar vein, 'great metalloclusters', was launched later by Rees [24] and appears to be surviving, e.g., in the work of the Drennan group on CO dehydrogenase as 'great clusters of biology' [6]. The quest for unifying principles in the catalysis of enzymes with unusual metal clusters is prevalent.

2.3. Hybrid clusters in other proteins

When the first crystal structural determination of an Hcp revealed that the 'prismane protein' does not contain a prismane cluster, the name 'hybrid cluster' was given to the novel 4Fe prosthetic group to denote that its structure contains both S^{2-} and O^{2-} bridges between the iron ions. This labelling raises the question whether such a combination occurs also in other metallocluster proteins either *sensu stricto* or under the broader definition of having two different bridges of any nature in metal clusters of nuclearity ≥ 4. Examples of the latter are readily found, e.g., in the Fe-S-Fe-C-Fe motif of the active site of nitrogenases [25,26], in the Fe-S-Fe-(CO)-Fe motif of the active site of Fe-Fe hydrogenases [27], or in the Cu-S-Cu-(OH)-Cu motif in the CuZ* form of the active site of nitrous oxide reductase [28,29]. The name hybrid cluster has thus far not been used in relation to these systems.

The narrower definition of sulfo and oxo bridges in 4Fe clusters applies, in addition to Hcp, to one other protein only: NiFe hydrogenases typically have, in addition to their NiFe active site, three electron transferring FeS clusters called proximal, medial, and distal with respect to their spacial distance from the active site [30]. The proximal FeS cluster in some NiFe hydrogenases is reversibly converted to an $Fe_4S_xO_y$ cluster upon inactivation by molecular oxygen. For example, when the O_2-tolerant [NiFe] hydrogenase from *Ralstonia eutropha* is crystallized aerobically, the proximal [4Fe-3S] cluster is found to have taken up an oxygen atom to form a [4Fe-O-3S] cluster. This, however, is not a hybrid cluster since the O atom is not bridging as it coordinates to a single iron only [31]. Only two cases have been described in which the proximal FeS cluster appears to form a genuine hybrid cluster under the action of molecular oxygen. In an early paper the [NiFe] hydrogenase of *D. desulfuricans* was reported to oxidatively convert its [4Fe-4S] proximal cluster into a [4Fe-3O-3S] hybrid cluster with two μ_2-O bridges [32]. A decade later essentially the same structure was found in the [NiFeSe] hydrogenase from *D. vulgaris* (Hildenborough) [33]. However, a few years later the structure was revised as [4Fe-3O-4S] [34], and in a yet more recent study to 1.3 Å resolution it was once more revised now into [4Fe-2O-4S] [35]. With this state of affairs my cautious conclusion would be that until today presumably only one hybrid cluster has been identified in addition to the one in the hybrid-cluster protein. Remarkably, the two HCs exhibit a striking structural similarity upon visual inspection (Fig. 3).

Zanello has attempted to make an inventory of what he calls 'hybrid iron sulfur proteins' encompassing six different HCs, namely, [4Fe-O-2S], [4Fe-O-3S], [4Fe-2O-2S], [4Fe-3O-2S], and two types of [4Fe-3O-3S] clusters [36]. I have the following misgivings. For [4Fe-O-2S] he cites our work [37], in which, however, we

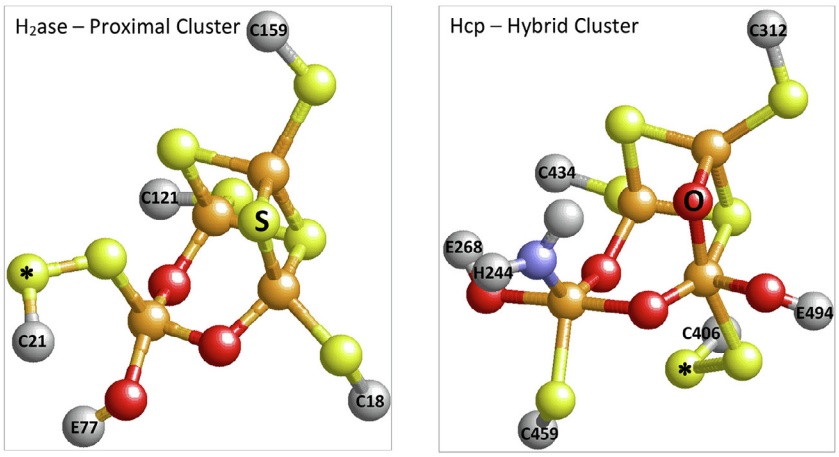

Fig. 3. Comparison of hybrid clusters in hydrogenase and in Hcp. The proximal cluster in *D. vulgaris* O_2-oxidized [NiFeSe] hydrogenase [4Fe μ_3S 2μ_2-S η_1-S 2μ_2O] is similar to the oxidized HC in *D. vulgaris* Hcp [4Fe μ_3-S μ_2-S η_1-S* 3μ_2-O]. A bridging sulfur in the one is replaced with a bridging oxygen in the other protein. Also, the persulfidocysteine coordinates to different Fe ions in the two proteins.

do not report such a cluster. Also, the [4Fe-O-3S] in *R. eutropha* [NiFe] hydrogenase is not an HC since there is no oxygen bridge [31]. Furthermore, the [4Fe-3O-3S] was initially claimed to be present in some hydrogenases [32,33], but this structure is probably in error [35]. Also, with reference to Hcp X-ray studies he claims [4Fe-O-2S] to differ from [4Fe-3O-3S], however, in one paper the persulfido S was not counted as part of the HC [38] while in earlier work it was included [39]. In other words, the two clusters are identical. Taken together, the inventory reduces to no more than the two HCs presented here in Fig. 3. As a final note, several of the ball-and–stick models in Zanello's review have direct Fe-Fe bonds [36] although direct metal–metal bonds are not known to occur in proteins.

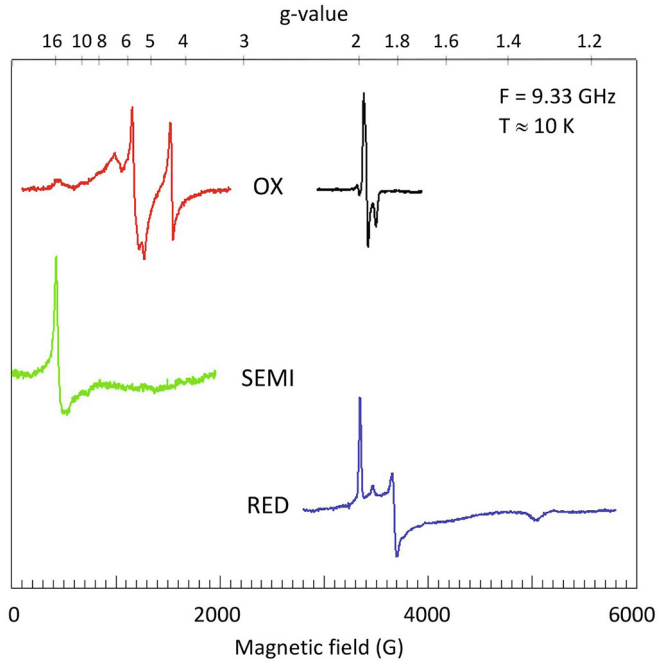

Fig. 4. EPR spectral signature of the hybrid cluster in *D. vulgaris* Hcp. The OX state of the HC is a mixture of two spin states, S = 9/2 (red) and S = 1/2 (black). One-electron reduction to the SEMI state affords an integer-spin system with S = 4 (green). A second one-electron reduction gives the RED state which is S = 1/2 (blue). Data replotted from [15].

3. Redox chemistry and paramagnetism

3.1. Multiple redox states and spin states of the hybrid cluster

The optical spectrum of iron-sulfur clusters in proteins is typically rather structureless, and the Hcp is no exception to this rule [12,15,40,41]. Their EPR spectroscopy thus gains a prominent place, and again the Hcp is no exception. Four redox states of the hybrid cluster have been identified with EPR, and they interconvert by three one-electron transitions. For reasons to be explained, below, I have recently proposed to name these states in increasing order of oxidation, respectively, 'reduced', semi-reduced' (or 'semi-oxidized'), 'oxidized', and 'super-oxidized' [42], which may be abbreviated as RED, SEMI, OX, and SUPER. The SUPER state has no EPR spectrum and therefore both clusters presumably are in a diamagnetic ground state, S = 0, at low temperature.

Fig. 4 gives an overview for *D. vulgaris* Hcp of the EPR spectral shapes of the other three forms on a single magnetic-field scale and with amplitudes normalized to unity. When purified aerobically the Hcp ends up in the OX state [1,40]. Anaerobic purification predominantly affords the SEMI state [37]. The RED state is obtained by reduction with, e.g., sodium dithionite [1].

Magnetically, the OX state is a mixture of half-integer high spin and low spin. Based on effective g values (17, 15.3, 9.7, 8.1, 6.65, 5.7–5.2) the high-spin signal has been assigned S = 9/2 [15]. The two spin states, S = 9/2 and S = 1/2 are not the components of a thermal equilibrium; their relative concentration has been estimated at 90% and 10%, respectively [15]. Physiological relevance of this spin mixture, if any, is unknown. All g values of the S = 1/2 system (1.968, 1.953, 1.903) are below that of the free-electron value g_e = 2.00232, which is common for iron-oxo but not for iron-sulfur clusters. Anaerobic purification or stepwise reduction of the aerobically purified Hcp in the presence of redox mediators gives the SEMI form, which should either have an integer spin or S = 0. The method of parallel-mode EPR, which allows for detection of integer spins, produces a single sharp line with an effective g value of 16 consistent with S = 4 [15]. Extended stepwise reduction or incubation with excess reductant produces the RED state, which is half-integer low spin, that is, S = 1/2. This is the signal (g = 2.004, 1.819, 1.32) that is reminiscent of the EPR of reduced synthetic prismane clusters [10]. A minor second S = 1/2 component is detected, e.g., as a small g_z on the high-field side of the main g_z peak.

The EPR spin-state assignment is corroborated by data from other spectroscopies. In particular magnetization curves as a function of temperature in magnetic circular dichroism (MCD) spectroscopy are consistent with the EPR observed high spins S = 9/2 and S = 4. The data suggest that the SEMI form may actually be a spin mixture of S = 4 and S = 0 [43]. Magnetic Mössbauer spectroscopic studies have also been found to concur with the EPR assignments of S = 4, S = 9/2, S = 0 for SEMI, OX, SUPER-OX, respectively [16,44,45]. In addition to being supportive of the EPR analyses Mössbauer spectroscopy has also provided the unique information that all four iron ions in the states SEMI, OX, and SUPER-OX have full valency, that is, they are Fe^{2+} or Fe^{3+}, and there is no delocalization into mixed-valence (sub)clusters of irons with formal fractional oxidation states [44,45]. The RED state has not been studied in detail because here the regular [4Fe-4S] cubane is reduced and contributes four paramagnetic irons, which complicates the Mössbauer analysis.

3.2. Iron redox chemistry in the hybrid cluster

Hcps have been subjected to stepwise reductive (with sodium dithionite) or oxidative (with potassium ferricyanide) titrations in the presence of a cocktail of mediators to approach redox equilibrium on a minutes time scale, with monitoring of the protein's redox states on the amplitudes of the EPR half-integer spin signals. The complete data set for three different Hcps is compiled in Fig. 5.

Pink colour signifies half-integer spins; gray is for integer (or zero) spins. The data have been fitted to the Nernst equation for one-electron transitions. The different redox states of the hybrid cluster have been labeled with the RED to SUPER-OX system and with the cluster-spin values, but also with the historical labeling scheme from "3+" through "6+". The latter is based on the assumption of the presence of a [6Fe-6S] core in the cluster, whereby S is 2- and so a fully oxidized core of six Fe(III) would have a charge of 6 + . Although this notation is now obsolete, as it bears no relevance to the actual structure of the hybrid cluster, it is still regularly found in contemporary literature on Hcp.

In addition to the data in Fig. 5, recently, EPR-monitored titrations have been reported for an Hcp from *Chlamydomonas reinhardtii*. These data have not been included in Fig. 5 because the report appears to be internally inconsistent: the reduced HC is claimed to have an EPR feature at g = 1.82, however, the presented spectra are devoid of such a signal (cf Fig. 4A, traces a and b in [46]).

Midpoint potentials (solid-trace amplitudes at 50%) can be seen to be similar for the three species. The transition at highest potential, ca 0.3–0.4 V, is probably too high to be of physiological relevance in strict, or facultative anaerobes, hence the naming SUPER-OX for the highest oxidation state. The other two transitions should be in physiological reach. The SEMI/OX transition in the *D. desulfuricans* Hcp has been measured on two different peaks (g_{eff} = 5.45 and 6.52) of the S = 9/2 spectrum, and they do not coin-

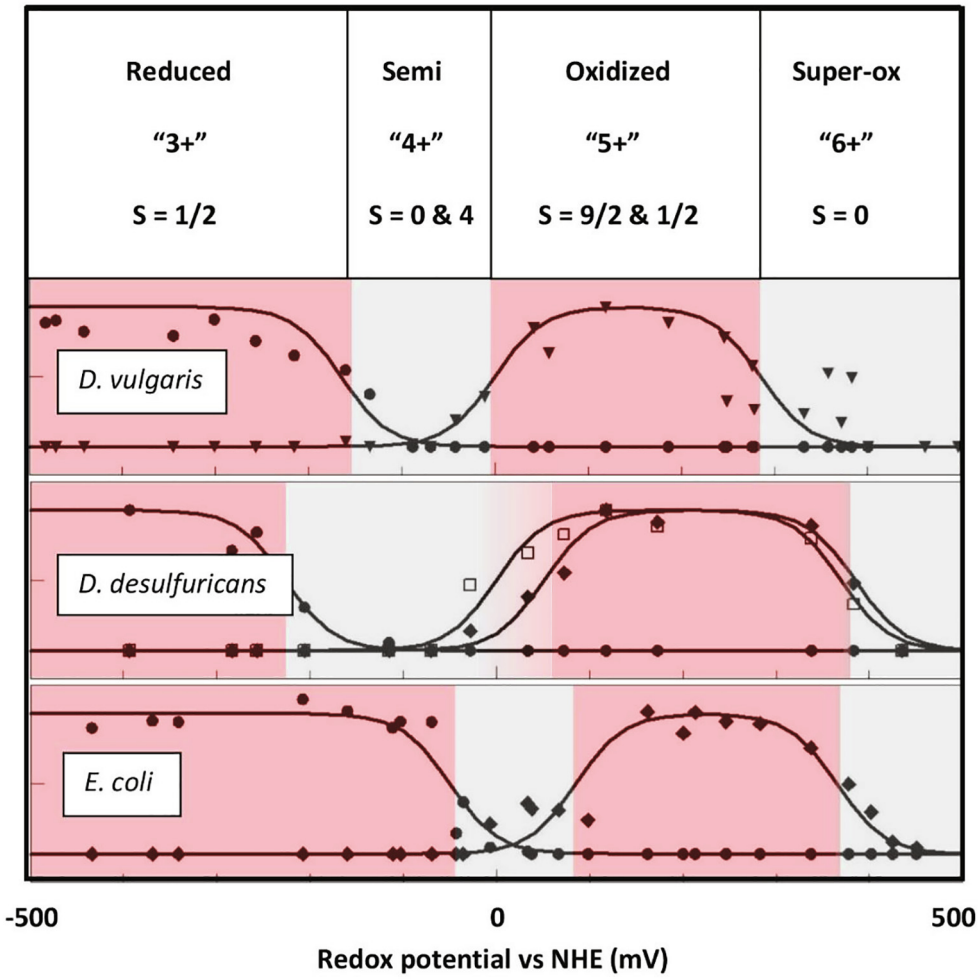

Fig. 5. EPR-monitored redox titrations of hybrid cluster proteins from three bacterial sources. Four redox states interconvert via three one-electron steps. Maximal amplitudes of EPR signals have been normalized to unit amplitude. Pink areas are from half-integer spins, gray areas represent integer or zero spins. Symbols are ●(S = 1/2 RED), ▼(S = 1/2 OX), □(S = 9/2 OX, g ≈ 5.45), ◆(S = 9/2, OX, g ≈ 6.5). Data are for Hcp from *D. vulgaris* [15], *D. Desulfuricans* [13], and *E. coli* [18].

cide, suggesting some heterogeneity. Generally, the data exhibit significant scatter indicating that approach to redox equilibrium with artificial electron donors/acceptors is slow. All data were taken with a 50 mM Hepes buffer at pH 7.5, and so there is no information on pH dependence of the reduction potentials.

3.3. Sulfur redox chemistry in the hybrid cluster

There is an elephant in the redox room and her name is sulfane sulfur. As discussed below, crystallography has revealed that a persulfido cysteine ligand to one of the irons in the OX and the SEMI form becomes a regular cysteine ligand in the RED state, whereas the extra sulfur turns into a μ_3-sulfide bridge between three irons. In other words, associated with the transition from SEMI to RED there is not only a one-electron metal-based reduction but also a two-electron sulfur-based reduction. Comments in the Hcp literature on this mechanistic enormity are distinctly scant. Tavares et al note that ".. the persulfido ligand .. may be involved in the redox behaviour of the cluster" [16]. Aragão et al. (including the present author) venture that ".. it cannot be excluded that at least one of the EPR-detected transitions is due to this process, and not to a reduction based on the iron atoms in the cluster" [5]. The latter proposal is of course incorrect: a two-electron process cannot be related to an integer-spin to half integer spin transition, and, furthermore, sulfur-atom redox chemistry, when involving a sulfur radical (S = 1/2), cannot be related to high-spin EPR. It is perhaps time to admit that there is a serious problem with the bookkeeping of the stoichiometry of reducing-equivalents (cf section 7).

3.4. Redox chemistry and spin of the electron-transfer cluster

Hcp contains two iron clusters: crystal structures of the proteins from *D. vulgaris* and *D. desulfuricans* show, in addition to the hybrid cluster, a regular [4Fe-4S] cluster. In hindsight this happened to be the most elusive cluster in the EPR analysis as its spectrum turned out to be not regular at all, escaping identification for a decade of intensive spectroscopic research. In redox terms the cluster is of the standard ferredoxin type, that is, in its oxidized state, with formally 2 Fe(III) and 2 Fe(II), it has a diamagnetic ground state, S = 0, at cryogenic temperatures. It can be reduced with one electron equivalent to the state with formally 1 Fe(III) and 3 Fe(II), whereupon its spin becomes half integer, S = n/2.

Fig. 6 gives EPR spectral shapes of the reduced electron-transfer cluster in *D. vulgaris*, *D. desulfuricans*, and *E. coli* Hcp [14,18]. The spectra from the sulfate reducers are very broad and their shape is unprecedented in metalloprotein EPR. In the figure the signal from the reduced hybrid cluster has been suppressed as much as possible by lowering the temperature to that of liquid helium and reducing its amplitude by partial power saturation and by overmodulation.

Signals similar to those of Fig. 6 trace a and b have previously been observed in reduced synthetic [4Fe-4S] model complexes, e.g., in $(Et_4N)_3[Fe_4S_4(S\text{-}o\text{-}C_6H_4StBu)_4]$, where they have been assigned to so-called quantum-mechanically spin-admixed S = 3/2 states, that is, to an S = 3/2 ground state that is coupled, presumably by spin–orbit coupling, to a very low-lying excited spin state. This unusual magnetism has been proposed to be associated with an idealized geometric deformation of the [4Fe-4S] core as schematically outlined in Fig. 7a (red arrows): the cube with Td symmetry, encompassing the intertwined 4Fe and 4S tetrahedra, is deformed, by compression along one of the S_4 symmetry axes, to D_{2d} symmetry, resulting in four parallel edges (Fe-S bonds) of shorter length than the remaining eight edges [47]. Checking the pdb files of the Hcps I find that this deformation is also operative in the oxidized cubane of the two *Desulfovibrio* proteins (pdb files 1GNT, 1W9M and 1GNL). In the reduced proteins (pdb files 1OA1 and 1OA0), in which the cubane is S = 3/2, the deformation is retained, however, there is an additional shortening of one of the other Fe-S bonds (blue arrows in Fig. 7a and blue number in Fig. 7b). Re-inspection of the work on the model compounds reveals that this extra deformation also occurs there (Fig. 7c). Taken all this together I draw two conclusions: (i) cubanes that exhibit an EPR spectrum indicative of a QM spin-admixed S = 3/2 are subject to a compressed tetragonal distortion both in model compounds and in metalloproteins; (ii) the overall distortion also includes an extra compression along one Fe-S bond perpendicular to the four parallel shortened ones. It would be interesting to know if this unusual connection between magnetism and geometry is of physiological relevance, for example, in the form of a reduction potential confined to a particular range of values. Unfortunately, perhaps due to the difficulty of measuring the broad EPR signal, redox titrations of the distorted cubanes have yet to be reported.

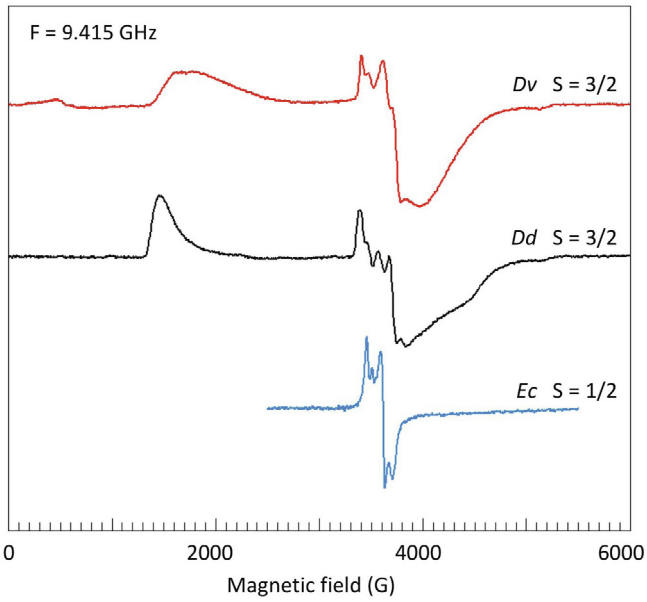

Fig. 6. EPR spectral signature of the electron-transfer cluster of three Hcp's. The upper two traces (S = 3/2 in *D. vulgaris* and *D. desulfuricans* Hcp) were taken at a low temperature of 4.2 K and a high microwave power of 80 mW to partially saturate away the hybrid cluster signal. The lower trace (S = 1/2 in *E. coli* Hcp) was taken at a temperature of 60 K to completely broaden away the hybrid cluster signal. Data are replotted from refs [14] and [18].

The spin-admixed cubanes are bound to the protein with the sequence $Cx_2Cx_8Cx_5CG$, and this motif is highly conserved in all Hcps from the three domains of life, except for the class of γ-proteobacteria, e.g., *E. coli*, whose Hcps bind their electron-transfer cluster with the sequence $Cx_2Cx_{11}Cx_6CG$. The EPR spectrum of the cluster in *E. coli* Hcp is given in Fig. 6, blue trace; it is the common S = 1/2 pattern with one g value above 2 and the two others below 2 characteristic of the majority of studied reduced [2Fe-2S] and [4Fe-4S] clusters. It was assigned to a [2Fe-2S] cluster [18] on the basis of its slow spin–lattice relaxation as evidenced from the absence of signal broadening up to 60 K [48]. However, several [4Fe-4S] clusters with comparable relaxation behaviour have since been found (e.g., [49]), which means that the cluster type has not been established by EPR. In fact, Pereira et al reported a stoichiometry of 8 ± 1 Fe per *E. coli* Hcp [17], which would be consistent with a [4Fe-4S] cluster next to the 4Fe hybrid cluster. Very recently, Fujihiro et al. have determined a crystal structure of *E. coli* Hcp, which, although carried out at a relatively low resolution of 3.6 Å, allowed them to conclude that to all likelihood indeed that electron-transfer cluster in this protein is also a [4Fe-4S] cluster [50]. Based on an EPR-monitored redox titration

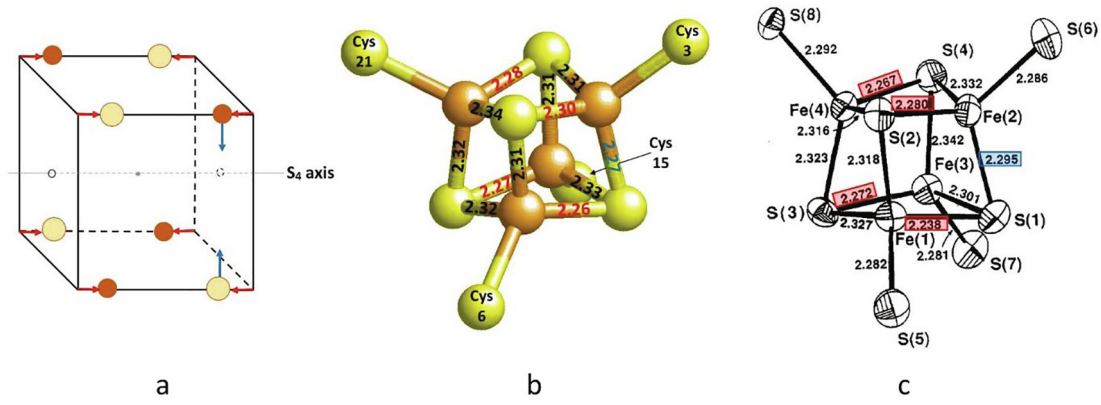

Fig. 7. Deformation of cubane cluster associated with spin admixed S = 3/2 EPR. (a) Schematic deformation of idealized cube made up of intertwined 4Fe and 4 S tetrahedra. The red arrows represent the deformation from T_d to D_{2d} symmetry proposed to be related to spin-admixed S = 3/2 EPR in certain synthetic clusters [47]. The blue arrows are an additional deformation found in Hcp's and also, in hindsight, retraceable in the early work on model clusters. (b) Cubane cluster in *D. vulgaris* Hcp with Fe-S bond length specified and shorter bond lengths indicated in red and blue. (c) Cubane cluster in model compound $(Et_4N)_3[Fe_4S_4(S\text{-}o\text{-}C_6H_4StBu)_4]$ with Fe-S bond length of the originally proposed deformation in red and an additional deformation in blue. This figure (c) was reprinted with permission from M.J. Carney et al., Inorg. Chem. 28, 1497–1503, Copyright 1989 American Chemical Society.

of *E. coli* Hcp a reduction potential of −35 mV at pH 7.5 has been reported, which is close to the potential of −50 mV for the RED/SEMI transition of the hybrid cluster [18].

4. Genetics of hybrid cluster proteins

4.1. Division of hybrid cluster proteins into classes

On the basis of systematic differences in their structural genes Hcps have been divided into three classes [18]. Class-I Hcps have the $Cx_2Cx_8Cx_5CG$ pattern to bind the electron-transferring iron-sulfur cluster and they have the overall polypeptide length of ca 550 residues found in the *Desulfovibrio* proteins. The structural gene is monocistronic, that is, it is not part of an operon. Facultative anaerobic gram-negative bacteria, in particular the *Enterobacteriales*, with *E. coli* as an example, encode class-II Hcps which have the $Cx_2Cx_{11}Cx_6CG$ cluster-binding pattern. The structural gene is part of the *hcp-hcr* operon, where *hcr* encodes the NADH-dependent hybrid cluster protein reductase, Hcr, which contains an FAD and a $[2Fe\text{-}2S]^{(2+;1+)}$ cluster. Class-III is a variant of class-I in which a stretch of ca 166 residues has been deleted from the sequence in between the two binding patterns for the iron clusters. The deletion corresponds to one of the two bundles of three antiparallel helices that in class-I make up the iron-sulfur cluster binding domain 1. Class-III Hcps occur in (hyper)thermophiles and form dimers [51].

It has recently been noticed that the grouping into classes I, II, and III is 'somewhat difficult' from a phylogenetic viewpoint since class II is at a higher clastidic level, being a Clade's subgroup, than the other two classes [46]. It should, however, be noted that the classification was originally intended to be of a structural nature, where later authors have used it in building simple phylogenetic trees [46,52]. In a further mix-up Han et al draw a phylogram which carries a branch called class-IV, encompassing certain eukaryotic Hcp sequences. Their class-IV branch has a sub-branch, now of a structural nature, exemplified by the parasite *Giardia lamblia*, where a 20-residue insertion is proposed to have occurred in the middle of the hybrid cluster binding motif [52]. Both proposals are questionable: the new branch has no structural definition and its level in phylogeny is undefined; regarding the sub-branch, in a CLUSTALW comparison under standard settings between the Hcps from *D. vulgaris* and *G. lamblia* I find the hypothetical 20-residue insert scattered into three fragments, and a 3D modelling of the *G. lamblia* protein on the basis of the crystal structure of the *D. vulgaris* protein places the scattered fragments peripherally away from the clusters.

All in all I suggest not to make too much of the division of Hcps into classes. In brief, there are two distinct binding motifs for the electron-transfer cluster, and there is a thermophilic, shortened, and possibly more stable Hcp version forming dimers. Note especially, that the class division has nothing to report on the structure of the hybrid cluster: all cluster-binding residues are fully conserved and there is no indication of significant divergence of the protein structure around the cluster.

4.2. Evolution of hybrid cluster proteins

It was noticed early on that the structural gene of Hcp exhibits significant sequence homology only with that of NiFe-containing CO dehydrogenase [18,53,54] in particular in the hybrid cluster binding region [8,37]. The Protein families (Pfam) database for classifying sequences into families and domains defines the Prismane / CO dehydrogenase family (PF03063) which at the time of writing includes 3159 sequences assigned to hybrid cluster proteins or to the beta chain of carbon monoxide dehydrogenase. The evolutionary relationship between the two enzymes is presently unclear. The binding motifs for the active-site clusters have similarity but are far from identical (see Fig. 8).

Thus, there are no rational grounds to suggest, as was recently done [55], that the product of an *hcp* gene is a candidate COdh enzyme. Also, the wrapping of the protein binding motif around the cluster is different in the two enzymes: in COdh the primary sequence maps onto the metal ions in a simple, linear fashion, while in Hcp the mapping is a complex knot of multiple ligation (Fig. 8).

The structure of the hybrid cluster and its direct protein surrounding appears to be remarkably conserved over all three domains of life as if Hcp was 'invented' only once and in subsequent times was judged by nature to be sufficiently adequate for its job as to obviate the need for evolutionary improvements. Consistent with this observation is the proposal that eukaryotic *hcp* genes are the result of one or two lateral gene transfer events from prokaryotes to anaerobic protists [56]. In fact, an extended analysis suggested multiple intra- and inter-domain *hcp* gene transfers [57]. Also, (repeated) internal gene duplication has been proposed [46].

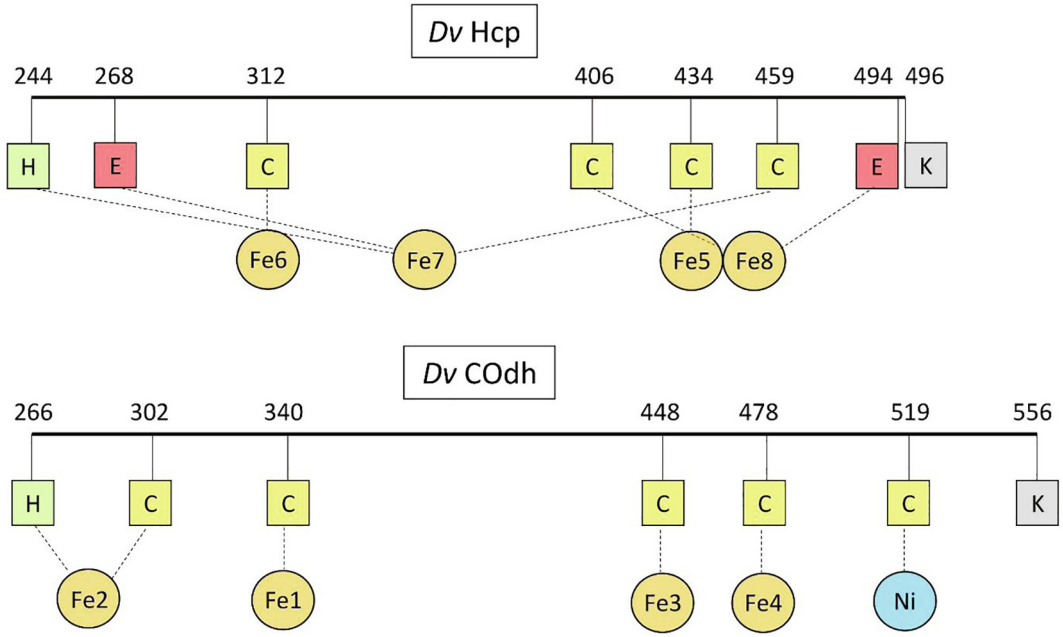

Fig. 8. Comparison of active-site cluster binding motifs in Hcp vs COdh. The two motifs are superficially similar, but differ significantly in their details. Residue numbering is for *D. vulgaris* Hcp, 1GNT.pdb [37], and for *D. vulgaris* COdh, 6B6X.pdb [6]. The conserved Lys496 in Hcp is in hydrogen bonding distance from a bridging oxygen [37]. The conserved Lys556 in COdh becomes a ligand to the nickel ion upon cluster oxidation [6].

4.3. Regulation of hybrid cluster protein expression

In *Desulfovibriones* expression of the *hcp* gene is under control of a transcription factor HcpR (regulator of *hcp* transcription) [58–62]. HcpR is a member of the Crp/Fnr family of global transcription regulators. The *hcpR* gene is typically found in the neighbourhood of the structural *hcp* gene (separated by 0–2 genes). The environmental signal for HcpR is nitric oxide or an NO producing molecule, e.g., nitrite. In *D. desulfuricans*, strain ATCC27774 the *hcpR2* gene encodes a 26.7 kDa protein that maturates as a dimer with a [4Fe-4S] cluster in each of the monomers. This dimer binds to a specific location on the DNA near the *hcp* gene and represses *hcp* transcription. The signal NO induces disintegration of the [4Fe-4S] cluster and the apo-protein can no longer bind to the DNA resulting in expression of the *hcp* gene [63,64].

In the unrelated anaerobe *Porphyromonas gingivalis* (Bacteroides) *hcp* expression is also under control of an NO sensing HcpR [65–68]. Molecular details are unknown.

In facultative anaerobe *E. coli* expression of the *hcp-hcr* operon depends on two separate signals. The global oxygen-responsive transcriptional regulator FNR (fumarate and nitrate reductase regulator) makes the general aerobic/anaerobic switch by acquiring a [4Fe-4S] cluster that is destroyed by oxygen. Under anaerobiosis the intact FNR binds to a target site upstream (centered at −72.5) from the *hcp-hcr* transcription initiation site [69]. In addition, there is an NO-responsive regulator NsrR (nitric oxide sensitive repressor) [59,69–73]. NsrR binds to the DNA near (+6) the *hcp-hcr* transcription initiation site [69].

Collectively the data indicate that a general mechanism for the regulation of expression of hybrid cluster proteins is effected by a specific repressive transcription factor whose iron-sulfur prosthetic group is labilized by nitric oxide.

5. Activities of hybrid cluster proteins

Four different activities have been reported for Hcps, in historical order: hydroxylamine reductase, peroxidase, nitric oxide reductase, and S-nitrosylase. The generic reaction equations are:

$$NH_2OH + 2[H] \rightarrow NH_3 + H_2O \quad (1)$$

$$H_2O_2 + 2[H] \rightarrow 2H_2O \quad (2)$$

$$2NO + 2[H] \rightarrow N_2O + H_2O \quad (3)$$

$$NO + protein - SH \rightarrow protein - SNO + [H] \quad (4)$$

I will now evaluate the possible physiological relevance of these reactions in the light of available microbiological, biochemical, and structural data.

5.1. Hydroxylamine reductase activity

Methyl viologen-dependent reduction of NH_2OH of *E. coli* Hcp was historically the first activity to be established for any Hcp [8]. By consequence in numerous databases Hcps are annotated as hydroxylamine reductase, although the activity is probably of little physiological relevance (below). The incitement to test for hydroxylamine reduction came from the observation that *Rhodospirillum rubrum* COdh acquired this activity when its NiFe-cluster ligand His-265 was substituted by valine [74]. The activity of *E. coli* Hcp obeyed Michaelis-Menten kinetics with V_{max} = 458 μ mol NH_2OH min^{-1} (mg protein)$^{-1}$ (i.e., $k_{cat} \approx 458$ s^{-1} for mw ≈ 60 kDa) and a K_M = 2.5 mM at pH 9.0 at ambient temperature. At the physiologically rather more realistic pH of 7.5 the activity dropped to 92 s^{-1} and the Michaelis constant increased to K_M = 39-mM. The latter value doesn't really strike one as an evolutionary success, and the authors concluded that 'other enzymatic roles for this enzyme cannot be dismissed at this time' [8]. Activity with the natural electron donor, the NADH-dependent Hcp reductase, has not been reported.

Methyl viologen-dependent reduction of hydroxylamine reported for other Hcps is typically some two orders of magnitude below that of the *E. coli* enzyme. *D. desulfuricans* Hcp has a V_{max} = 3.6 when measured with 100 mM NH_2OH in the pH range of 7.0–8.8 at ambient temperature [5]. *R. capsulatus* Hcp has V_{max} = 3 and K_M = 1-mM at pH 9.0 and 40 ^{0}C [41]. Hcp from the hyperthermophile *P. furiosus* has V_{max} = 4.5 and a K_M = 0.4 mM at pH 9.0 and 70 ^{0}C

[51]. Taken together it appears that the hydroxylamine reductase activity of *E. coli* Hcp is probably an accidental, promiscuous, rather than a physiologically relevant activity.

This conclusion finds further support in the long-known fact that hydroxylamine reduction is a common side activity of several other enzymes present in the relevant species. It was, for example, reported 60 years ago that the NADPH-dependent sulfite reductase in *E. coli* exhibits hydroxylamine reductase activity at pH 9.0 that is an order of magnitude higher than the bacterial intrinsic sulphite reductase activity at pH 8.0 [75]. The observation has been reinforced several times [76,77]. Similar results have been reported for the preponderant sulfite reductase of *D. vulgaris* [78]. In this light it doesn't seem to make sense to synthesize yet another complex enzyme (Hcp) to exhibit a poorer version of this activity. It is perhaps time, in contrast to recent literature [79,80], to remove 'hydroxylamine reductase' from the databases as 'the' activity of hybrid cluster proteins.

5.2. Peroxidase activity

When Almeida et al. [9] found that expression of the *hcp* gene in *E. coli* was upregulated under the influence of H_2O_2 and that this induction was regulated by the redox-sensitive transcription factor OxyR they hypothesized that Hcp might play a role in oxidative stress protection. With sodium ascorbate as the electron donor a low peroxidase activity was found: V_{max} = 0.17 μmol H_2O_2 reduced min^{-1} (mg protein)$^{-1}$, and K_M (H_2O_2) = 0.3 mM. For *D. desulfuricans* Hcp the numbers were V_{max} = 0.05 U·mg^{-1} and K_M = 0.3 mM. These very low activities made the authors express that 'this suggests that the true physiological substrate is not known' and that 'the physiological reductant for either Hcp was not available, further hindering a correct enzymatic assay' [9]. Furthermore, excess addition of H_2O_2 to *D. desulfuricans* Hcp had no detectable effect on the EPR spectrum of the OX or the RED form. To put the numbers in perspective note that, e.g., cell-free extract from *D. vulgaris* already has a peroxidase activity that is two orders of magnitude higher [81] than the value reported for the purified *D. desulfuricans* Hcp. The rubredoxin-rubrerythrin system is likely to be a major contributor to this activity [82]. The proposal of Hcp peroxidase activity has not led to any follow-up studies except for a vague allusion to involvement in defense against reactive oxygen species production [83].

5.3. Nitric oxide reductase activity

Following their observation that *hcp* expression in *E. coli* is under the NO-sensing regulator NsrR [71] Cole and collaborators set out to characterize NO reductase activity of the Hcp [3,84]. They constructed a mutant that lacked the known NO reductases NorVW and flavohemoprotein (flavoHb or Hmp). While anaerobic growth of this mutant was virtually insensitive to repeated additions of 1 μM NO, growth of its *Δhcp* derivative (that is, *hcp* deleted) was almost completely inhibited by 1 μM NO. The *hcp*$^+$ strain stoichiometrically converted 2NO into N_2O. Purified Hcp also actively reduced NO but remarkably, and hitherto unexplained, only if isolated and purified as an integral complex with its reductase Hcr. A mixture of separately purified Hcp and Hcr was devoid of activity [3]. Future studies should address this unusual observation.

Enzyme kinetics were analysed in whole cells and in 80% purified Hcp-Hcr complex in terms of straightforward Michaelis-Menten kinetics. Whole-cell studies afforded a K_M (NO) = 575 nM, and with this number the catalytic efficiency (or: specificity constant, kinetic efficiency) k_{cat}/K_M for the purified Hcp-Hcr complex was calculated to be 2400 × 10^6 M^{-1} s^{-1}, which made the authors to conclude that they "have shown that Hcp-Hcr is the major reductase activity at very low concentrations of NO" [3]. I have previously expressed concern over the reported value of the catalytic efficiency because it exceeds the approximate value of 10^8-10^9 M^{-1} s^{-1} generally assumed to be the diffusion-controlled limit of any enzyme activity [42]. The number is possibly the result of a calculation error. The authors report a V_{max} = 2390 nmol NO reduced s^{-1} (mg protein)$^{-1}$ [3]. Taking a molecular weight of ca 97.5 kDa for the holo-proteins Hcp + Hcr, the reported V_{max} translates into a k_{cat} = 2.39 μmol NO s^{-1} (1/97.5 μmol enzyme)$^{-1}$ = 233 s^{-1}. Using this number the catalytic efficiency is reduced by an order of magnitude to ca 4 × 10^8 M^{-1} s^{-1}, which now is a possible, but still an extremely high value.

So where is the catch? I suggest a critique of the model chosen to fit the kinetic data. Girsch and De Vries have formulated a minimal scheme for the reaction in which an enzyme has to bind two identical substrate molecules in which the K's are dissociation constants [85]. This leads to the rate equation for NO reduction

$$v = k_{cat}[E_{Total}] / (1 + K_2(1/[NO] + K_1/[NO]^2) \quad (5)$$

Using this equation for the analysis of Hcp activity in whole cells Wang et al found that in a fit to their data K_1 converged towards zero "thus resulting in a simple Michaelis-Menten model $V = V_{max}/(1 + K_2/[NO])$" [3]. In other words K_2 is equal to the K_M. I have previously noted that K_1 = 0 would imply the physical impossibility of an infinitely strong association between Hcp and the first NO to bind [42]. For additional insight I have now re-analyzed some of the original data of Wang et al. using the proper equation (5). The data are reproduced in Fig. 9 with the Michaelis-Menten fit in red giving K_M = 384 nM (and K_1 = 0). Two other fits, now on the basis of Eq. (5), are in green (K_1 = 10 nM, K_2 = 190 nM) and in blue (K_1 = 100 nM, K_2 = 39 nM). The three fits have unweighted mean square errors of 0.68, 0.70, and 0.76, respectively. So the Michaelis-Menten fit is the best by a smidge, but its underlying

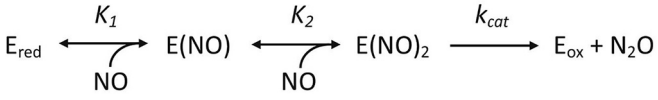

Scheme 1.

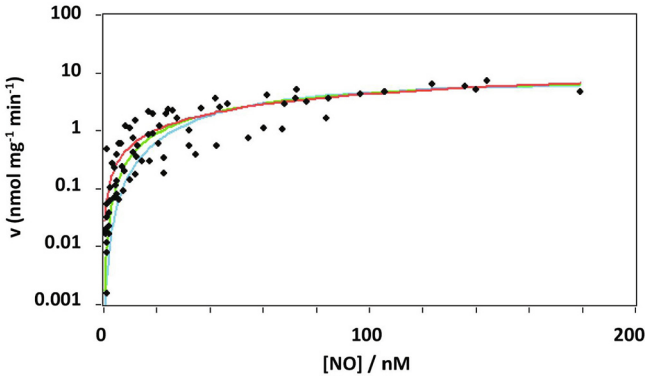

Fig. 9. Kinetic analysis of NO reductase activity by Hcp in *E. coli* cells. The data points have been read out from Fig. 7B of [3] and replotted. The used strain JCB5210 is devoid of NO reductases NorVW and Hmp, so the data should reflect activity of Hcp only. Three fits are shown to the data. The red trace is a straightforward Michaelis-Menten fit as proposed by Wang et al. [3], here with K_M = 384 nM. The other two traces are fits according to Scheme 1 with K_1 = 10 nM, K_2 = 190 nM (green) or K_1 = 100 nM, K_2 = 39 nM (blue). It is concluded that the quality of the data do not allow for a discrimination between the three fits; the model of the red trace is physically impossible.

mechanism is also physically impossible. The other two fits indicate that the two dissociation constants (i.e. not K_M) are in the nanomolar range but the quality of the data is insufficient to determine their relative and absolute magnitude.

All in all Cole and collaborators have convincingly shown that expression of Hcp in *E. coli* is induced by NO (which has been confirmed in recent studies [86–88]), and that NADH-dependent Hcp-Hcr complex is an NO reductase apparently with respectable, but not exceptionally high activity. The enzyme's affinities for NO are in the nanomolar range, but a K_M is undefined and there is, therefore, in this case no such thing as a catalytic efficiency in terms of Michaelis-Menten kinetics.

The natural electron donor for *D. vulgaris* Hcp is not known. With dithionite-reduced benzyl viologen and with high NO concentrations a modest NO to N_2O reduction activity is detected against a significant background of chemical reduction [42].

5.4. S-nitrosylase activity

Stammler and collaborators have reported that anaerobic growth of *E. coli* on nitrate leads to S-nitrosylation of transcription factor OxyR by NO produced by nitrate reductase, which result in de-repression of expression of the *hcp* gene and, to a lesser extent, of the *hcr* gene [89]. In a subsequent proposal they envision Hcp to auto S-nitrosylate as the initial event in a signal cascade, through S-nitrosylation, of a large number of interdependent proteins, or Hcp interactome, thus conferring, e.g., enhanced motility and protection against nitrosative stress [4]. Criticism has been ventured by the present author on mechanistic grounds [42] and more recently, and more extensively, in a review by Cole on physiological grounds [90].

A major conclusion of the Stammler group is that *E. coli* Hcp is an SNO synthase and protein S-nitrosylase [4]. The term 'SNO synthase' is new and not defined, but inspection of the paper's graphical abstract suggests that it is identically equal to auto-S-nitrosylase. That latter activity is also not unproblematic: the authors suggest that NO first binds to a cluster iron and subsequently is transferred to a cysteine residue, whereupon the formed Hcp-SNO can S-nitrosylate other proteins. Since none of the free Cys residues is found to be nitrosylated, they propose that it is a cluster–ligand Cys that takes up NO and becomes one-electron oxidized. No evidence is presented to support the idea that it is possible for the hybrid cluster to detach one of its Cys ligands without cluster disintegration. As a matter of fact, in *D. desulfuricans* the Cys428Ser mutant of Hcp (Cys434 in *D. vulgaris* Hcp) has lost the hybrid cluster completely [14]. And Ser substitution for any of the four Cys coordinating the cubane cluster in *D. vulgaris* Hcp leads to a protein that does not fold [2]. Furthermore, my EPR studies show that incubation of *D. vulgaris* Hcp with NO in absence of electron donors/acceptors semi-quantitatively leads to dinitrosyl iron derivatives of the hybrid cluster [42]. Seth et al. also propose that in the *E. coli* Hcp-Hcr system the electron that is released upon S-nitrosylation of a cysteine is eventually (presumably after two cycles) taken up by NAD^+ [4]. However, the lowest reduction potential of Hcp, i.e. the SEMI/RED potential (Fig. 5) is several hundred millivolt less negative than the NAD^+/NADH potential of −320 mV which makes the proposed electron transfer thermodynamically impossible in absence of an external energy source. Seth et al. further propose that *E. coli* Hcp undergoes disulfide bridge formation as part of the signalling process [4]. How this occurs and what the underlying redox chemistry is remains obscure. Finally, but importantly, Cole has pointed out that the experiments of Seth et al. on whole cells have been carried out under physiologically unrealistically high NO concentrations [90]. Also, in their experiments on isolated Hcp the authors have incubated with considerable excess of NO [4].

It is not impossible that Hcp transfers NO directly to other proteins, i.e., that its transnitrosylase activity is actually a non-redox NO transferase activity. It is not even impossible that the Hcp-Hcr system would be the cause of true S-nitrosyl formation on other proteins, but this would require an electron acceptor other than NAD^+. Taken the above together the unavoidable conclusion must be that the proposed signalling role of Hcp at this time is interesting but at the same time highly speculative as well as highly controversial. Any notion of this controversiality is not yet apparent in recent literature [91–98] with an occasional exception [99].

6. Mechanics of the hybrid cluster

6.1. Redox structural changes in the hybrid cluster

High-resolution crystal structures in different redox states have been determined for the Hcps of *D. vulgaris* and *D. desulfuricans* [2,5,37–39,100,101] (and a low-resolution structure was very recently reported for the *E. coli* Hcp [50]). When the protein is purified aerobically the hybrid cluster ends up in the OX state (cf Fig. 5). The SEMI state is predominantly obtained after purification and crystallization under anaerobic conditions. Crystal structures of the RED state have been determined on protein anaerobically purified and crystallized and subsequently soaked in a solution of reductant dithionite. Structures of the hybrid cluster in the OX and SEMI state of *D. vulgaris* Hcp are identical except for a μ_2-bridging oxygen, O10 (see Fig. 2) which in the OX state is disordered between two positions around the single position it takes in the SEMI form [38]. Physiological significance of this disorder, if any, is unknown.

In Fig. 2 the structures of the hybrid cluster are compared in the OX/SEMI vs the RED form. Of the coordinating amino acid side chains only the ligand atom and the next carbon are shown. The numbering of cluster atoms is taken from [5,37]. In the RED state the three μ_2-oxo bridges have disappeared; there is now a single oxygen labelled Y to indicate that its relation, if any, to the O's in the OX structure is unknown. Structure of the cluster as a whole in both states is highly irregular. The only sub-structure with regularity is the (Fe5, S5, Fe6, S6) diamond, which is reminiscent of [2Fe-2S] clusters or of a side plane of a [4Fe-4S] cubane or a [6Fe-6S] prismane. A key difference between the two states is that the RED structure is open and the OX structure is closed, as if the RED structure is ready to accept a substrate while the OX structure has closed up after getting rid of a product. Arguably the most stunning aspect of the comparison is the considerable, but localized, structural change that comes with reduction: the Fe_2S_2 diamond essentially remains in place and so does the position of Fe7, however, Fe8 makes a move over ca 2 Å. The most drastic change, in terms of position as well as coordination is for the end-on S7 of persulfidocysteine-406. It detaches from the side chain, moves over ca 4 Å, and turns from η_1-ligand of Fe8 into a μ_3 bridge of Fe5, Fe7, and Fe8. Since residue 406 has now turned into a regular cysteine coordinating Fe8, the overall change of S7′s move is associated with an electron-pair reduction process that comes on top of the one-electron metal-based reduction. The nature of oxygen Y in the RED structure is uncertain. In the *D. vulgaris* Hcp the distance between Y and Fe7 is 2.77 Å, which may qualify as a very weak bond, however, in the *D. desulfuricans* Hcp this distance is 3.13–3.16 Å. In both structures Y is in hydrogen-bonding distance (2.92 and 2.88 Å respectively) from the NH_3^+ group of conserved residue Lys496.

Either in hindsight or contemporaneously with the first crystallographic studies, multiple spectroscopic observations were found to be consistent with the X-ray determined structure of the hybrid

cluster. Nitrogen ligation was inferred from linewidth changes in multi-frequency EPR [15]. Electron spin echo envelope modulation (ESEEM) spectroscopy was consistent with a histidine ligand [14]. Resonance Raman spectroscopy suggested an oxygen ligand [102], more specifically a solvent-exchangeable oxygen bridging between Fe7 and Fe5 [2]. Extended X-ray absorption fine structure (EXAFS) spectroscopy data were consistent with the presence of an FeS_2Fe diamond sub-structure, with two different Fe-Fe distances of ca 2.7 and 3.1 Å, respectively, and with the absence of a long 3.8 Å Fe-Fe distance found in prismanes [2]. Contributions from EPR, MCD, and Mössbauer spectroscopies in delineating the magnetic properties of the hybrid cluster have already been outlined, above.

6.2. The pinball mechanism of product release

Reading out redox-dependent structural changes by comparison of crystallographic structures in two redox states has an aspect of arbitrariness in the choice of how the two structures are superimposed in a single 3D space. A common approach is to minimize the sum of all squared distances between corresponding atoms of the protein's main chain structures, as was done in [5] for the RED and SEMI structures of *D. desulfuricans* Hcp to elucidate the movements of Fe8 and the Cys399 persulfido S7. However, normalizing on protein atoms may suppress and thus obscure possible local protein movements associated with the structural transformation of the hybrid cluster. In *D. vulgaris* Hcp, since Fe8 is not only coordinatively bound to Cys406, but also to Glu494, and possibly, via oxygen 'Y', to Lys496, I have normalized the 3D positions of the hybrid cluster in the RED and SEMI structures by minimization of the distances between the corresponding iron positions other than Fe8, that is, on Fe5, Fe6, and Fe7. The overlay presented in Fig. 10, shows only minor variations in the Fe_2S_2 diamond and the sulfurs of its two Cys ligands and a virtual invariant structure for the (N, O, S) coordination of Fe7 by His244, Glu268, and Cys459. In contrast, the movements of Fe8 and S7 are found to be associated with considerable movement not only of the sulfur (s) of Cys406, but also of the coordinating oxygen of Glu494. On the other hand, the nitrogen of Lys496, hydrogen bonding to oxygen 'Y', hardly moves. In other words, the closure of the hybrid cluster, in going from the RED to the SEMI structure is a concerted local event involving predominantly four atoms, as indicated in Fig. 10, reminiscent of the movement of a flipper in a pinball machine.

Then what is the 'ball' that has to be expelled from the hybrid cluster? When *D. vulgaris* Hcp with its hybrid cluster in the OX form (that is, structurally equivalent to the SEMI form) is incubated with excess N_2O, no spectral changes whatsoever are observed in its EPR spectrum. The same experiment, however, carried out with the cluster in the RED form affords considerable changes in the EPR spectrum (Fig. 11), which can be taken to attest to the fact that the nitrous oxide molecule is not only able to reach and bind to the hybrid cluster, but also to significantly affect its structure [42]. At first sight this observation is unexpected where N_2O is the product of the NO reductase reaction and Hcp in the RED form is supposed to be the enzyme ready to bind its substrates, that is, two molecules of NO. Apparently, the RED hybrid cluster is 'open' enough to accommodate the product N_2O, be it with low affinity, while the OX cluster is sufficiently 'closed' to block access of N_2O. The following hypothesis naturally presents itself: since Hcp has a high affinity for its gaseous substrates 2NO, it may well have a similarly high affinity for its structurally not so different gaseous product N_2O. In order for the catalysis not to stall, the pinball movement is required to kick out the product and to close up the active site in order to prevent futile rebound.

6.3. Comparison with the NiFe cluster of CO dehydrogenase

Hybrid cluster proteins and NiFe-containing carbon monoxide dehydrogenases show significant sequence homology in particular in the part that coordinates the active-site cluster. Also the shapes of the hybrid cluster and the NiFe cluster exhibit similarity in that both are made up of an incomplete cubane bridged to an 'external' iron ion (in CO dehydrogenase literature called 'unique Fe'), cf [2] vs [103,104]. In both enzymes this cluster undergoes redox-dependent structural changes involving the breaking and making of several coordination bonds associated with movement of atoms over considerable distances (cf ref [5] vs [6]). In search for a unifying principle of action one would be tempted to compare the details of these flexible clusters. Unfortunately, this comparison is presently not yet possible because the crystallographically doc-

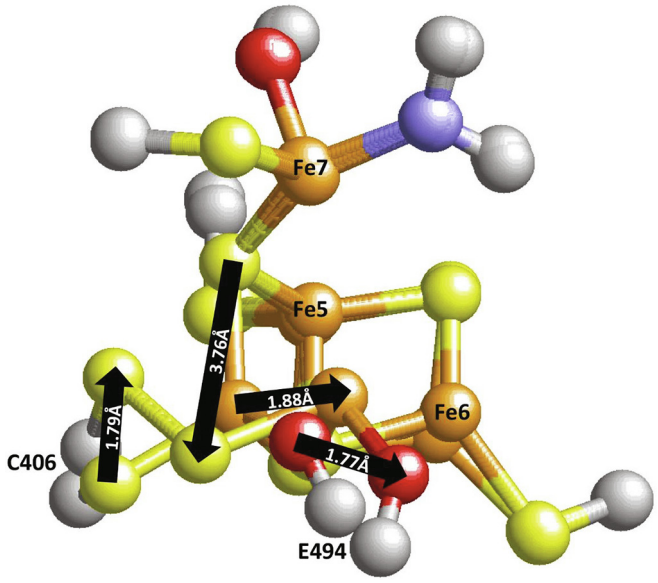

Fig. 10. Concerted movement in the RED to SEMI/OX state transition of the HC in *D. vulgaris* Hcp. Overlay of the core cluster structures was effected by mutual anchoring on Fe5, Fe6, and Fe7 to emphasize the movement not only of Fe8 and S7, but also the side chains of residues Cys406 and Glu494 that coordinate Fe8. The complex overall movement is given the name 'pinball mechanism'; its function is proposed to be the forced release of product N_2O.

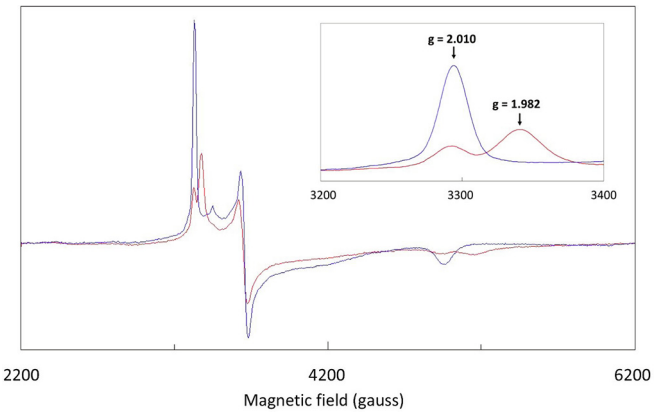

Fig. 11. Product N_2O binds to the RED state of the HC in *D. vulgaris* Hcp. The EPR spectrum of the reduced HC, with g = 2.010, 1.823, 1.34, is partially converted into a new spectrum with g = 1.982, 1.823, 1.29 upon flushing the protein solution for 1 min with nitrous oxide. The figure was reproduced from ref. [42].

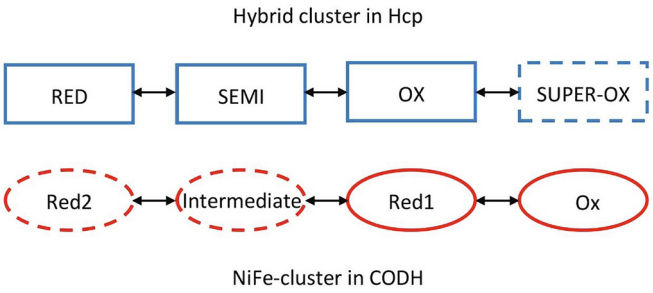

Scheme 2.

umented structural changes in the two enzymes apply to mutually incomparable redox states.

Scheme 2 summarizes the fact that the active-site cluster in both enzymes can occur in four different redox states [15,105], where the three states on the low-potential side are considered to be involved in the two-electron associated substrate conversion. The state on the high-potential side in Hcp is considered physiologically irrelevant [2]; in COdh it has been proposed to be a cluster state that is protected from O_2 damage [6]. In Scheme 2 solid enclosing lines indicate that the state has been characterized crystallographically; broken lines indicate that the protein with the cluster in the indicated state has not been crystallized yet. Scheme 2 tries to make apparent what is somewhat veiled by the different nomenclature used for the redox states of the two proteins, namely, that only one cluster state has been structurally determined for both enzymes. The cluster structural change in COdh is for a redox transition that has not been characterized in Hcp, and vice versa. A meaningful comparison would require a crystal structure of COdh with the NiFe cluster fully reduced, that is, in the Red2 state.

7. Hybrid cluster mechanism of action

EPR and Mössbauer spectroscopies have pinned down the hybrid cluster to occur in four redox states connected by iron-based single-electron transitions and with no fractional iron valencies in the three most oxidized states. Tying together this redox chemistry of the HC, its activity as an NO reductase (with stoichiometric reduction of two NOs to one N_2O), its switching between open and closed structures, its binding affinity for N_2O when reduced and the absence thereof when oxidized, the enigmatic behaviour of its three oxygen bridges that disappear upon full reduction, and above all its hitherto unaccounted for redox chemistry associated with the persulfidocysteine, let us be daring and put forth, in Scheme 3, a first elementary proposal for a reaction mechanism of Hcps, not to be cast in stone but as a road map that suggests future experiments.

States that have been characterized in protein crystallography are marked with a thick dark grey surrounding line. The key assumption in Scheme 3 is that there are two basic configurations of the hybrid cluster: an open one and a closed one (cf Fig. 2). The transition from open to closed is associated with the pinball movement of sulfur S7 and iron Fe8 (and, not shown here, the protein in the form of Cys406 and Glu494 in *D. vulgaris* Hcp counting). Importantly, this transition brings along an intra-cluster re-distribution of two electrons in which S7 becomes a part of a persulfido side chain (indicated in the Scheme as S7*) and Fe7 and Fe8 concomitantly become reduced to ferrous.

A complete catalytic cycle follows the five solid black arrows in the lower part of Scheme 3. Starting point is the hybrid cluster in the RED state with open configuration, that is, the RED structure of Fig. 2. Two NO molecules sequentially bind to Fe7 (where binding to a single iron is indicated by EPR spectroscopy [42]) and are converted to N_2O with two iron-based electrons (lighter color indicates higher Fe oxidation state). Release of the product N_2O is mandatorily coupled to a pinball switch into a closed configuration, in which S^0 is shorthand for Cys406 turning into a persulfido ligand to Fe8. The open state is re-gained by two-electron redistribution, and two subsequent one-electron reductions (via the cubane and an external electron donor) regenerate the free enzyme.

In the RED state the two irons in the Fe_2S_2 diamond are presented as a mixed-valence pair with individual formal charge of 2.5 + rather than as a charge-localized Fe^{2+}-Fe^{3+} pair. There is presently no direct experimental evidence to support this view, except that HCP got its original 'prismane protein' name from a remarkable correspondence between its EPR spectrum in the RED state and the spectrum of the $[6Fe\text{-}6S]^{3+}$ core in synthetic prismanes [10]. The [6Fe-6S] core can be viewed as constructed from three [2Fe-2S] diamonds, and its Mössbauer spectrum indicates full charge delocalization with formally six $Fe^{2.5+}$ ions [10].

At the top of the Scheme green broken arrows indicate subsequent oxidations that afford closed configurations of the crystallographically characterized SEMI and OX states and, finally, (not shown in the Scheme) the spectroscopically described SUPER-OX state. The RED to SEMI reaction has been labelled 'slow' since it has thus far only been achieved by prolongued incubation (typically 10 min.) with excess dithionite. The kinetics of the reaction have not been studied yet. The reaction is associated with the release of two bridging oxygens possibly as H_2O molecules as suggested by the observation an Fe-O stretch frequency in resonance Raman spectroscopy that is solvent exchangeable in an $H_2^{16}O$/$H_2^{18}O$ experiment [2,102].

On the basis of Scheme 3 we can now formulate specific questions to be addressed in future research. Clearly, a key issue is the affinity of the product N_2O for different HC states, that is, whether the RED-closed state is really part of the catalytic cycle as a requirement to push out N_2O, or whether it is not, in which case the cycle takes the shortcut indicated in the Scheme with a red broken arrow. Addressing this question requires pre-steady-state experimentation because according to Scheme 3 neither this intermediate nor the previous OX-open-N_2O state can be build up in steady state, and thus each would have a lifetime of less than the time span of a single enzyme turnover. A related point is whether there is a direct redox route to the SEMI-closed state from the RED-closed state either as a reaction cycle intermediate or as an intermediate in the slow oxidation of RED-open. Both questions address the fundamental role of the S7 persulfido form of Cys406 in Hcp: is it central to catalysis and/or is it part of an oxidative rearrangement to protect the protein in an aerobic environment?

Scheme 3 also predicts that the OX-open state can be build up, namely, by incubating HCP with the HC in the RED-open state with two-fold excess of NO but in the absence of external electron donors. Possibly, one electron will be transferred from Hcp's [4Fe-4S] cluster before steady state is reached. This stable intermediate should be amenable to spectroscopic and possibly even crystallographic analysis.

Furtehrmore, an inquiry into the nature of the Fe-NO bond(s) is suggested. Are the NOs bound to Fe7, to Fe8, or to both? And is there cooperativity in their binding? Spectroscopically monitored pre-steady-state experimentation once more appears to be the way to go, now combined with variable initial NO concentrations.

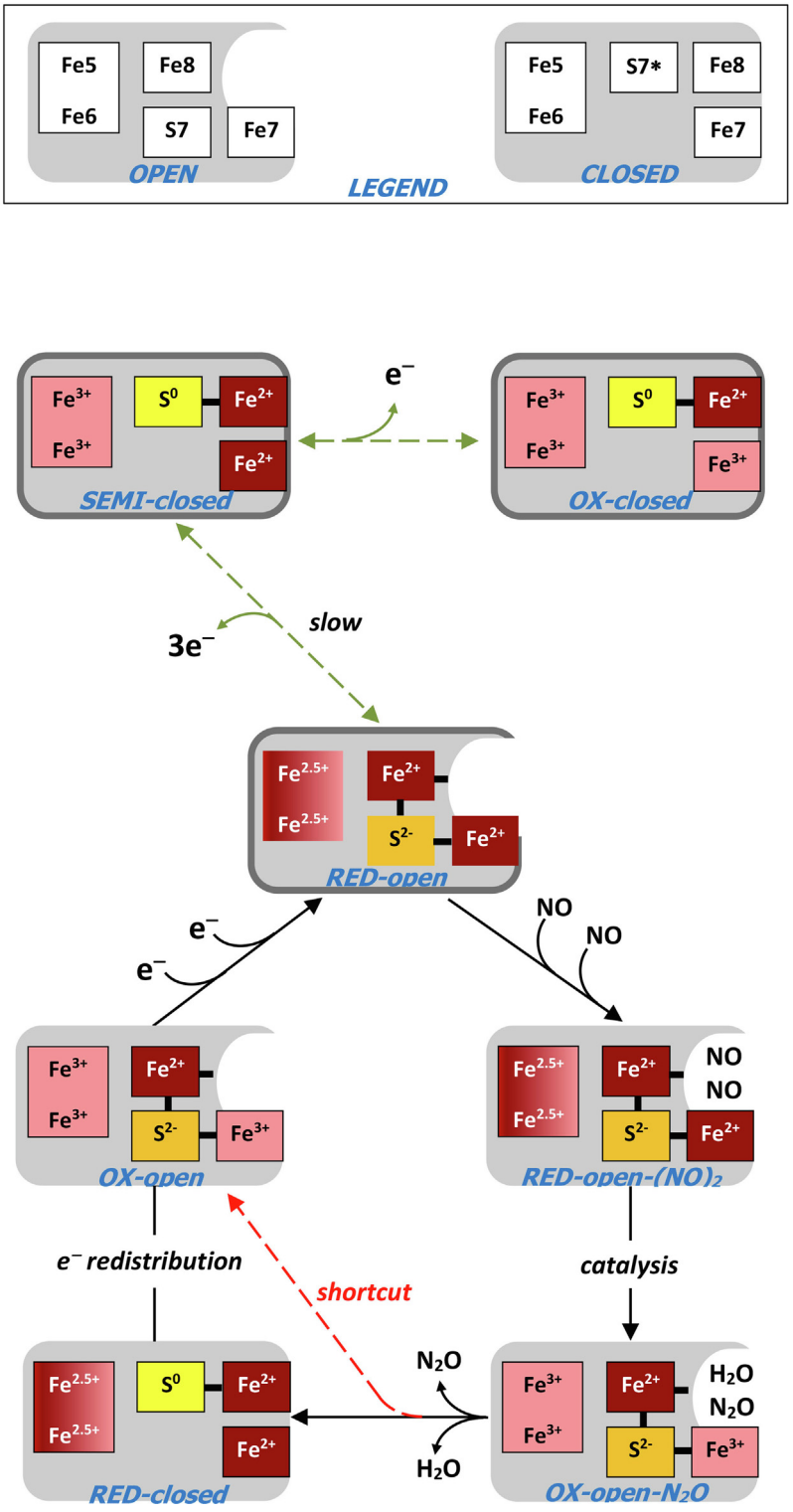

Scheme 3.

8. Concluding remarks

Some 33 years down the line of the first observation of a protein with a prismane-like EPR spectrum it is now firmly established that the hybrid cluster protein of bacteria (and presumably also of archaea and monocellular eukarya) is a nitric oxide reductase. Whether it also functions in signal transduction by means of some form of transnitrosylation remains to be rigorously tested. The enzyme contains two prosthetic groups, a one-electron transferring iron-sulfur cluster and an active site iron-sulfur-oxo hybrid cluster. The latter has an unprecedented, complex structure whose core in the oxidized state may be described as [4Fe μ_3-S μ_2-S η_1-S* $3\mu_2$-O], in which S* stands for the coordinating sulfur of a persulfido cysteine, and in the reduced state may be described as [4Fe $2\mu_3$-S μ_2-S (O)], in which the parentheses indicate that the status of an oxygen as a ligand is presently not clear. The hybrid cluster

undergoes two metal-based one-electron transitions in a potential range that is considered to be physiologically relevant. Each of the states involved, OX, SEMI, and RED, has very characteristic EPR spectroscopic properties. Reduction is associated with a drastic structural rearrangement of part of the hybrid cluster, which specifically involves redox chemistry of a sulfur atom. This two-electron transition should be included in any description of the enzyme's catalytic mechanism, which has been attempted in the present review for the first time. Hybrid cluster proteins show significant sequence and structural homology with the enzyme carbon monoxide dehydrogenase in particular in the structure of the hybrid cluster versus the NiFe-cluster. Whether this homology has any mechanistic implication is presently still difficult to evaluate for lack of a crystal structure of COdh in the fully reduced Red2 state. With a solid body of knowledge on hybrid cluster proteins now available in terms of structure, spectroscopy, biochemistry, genetics, and microbiology the time appears right for a serious research effort into elucidating the enzyme's mechanism of action. The first bits of information have already been obtained in an EPR spectroscopic study of equilibrium incubations with substrate and product. The next leap will require fast kinetics methodology to identify and characterize short-lived enzyme intermediates in pre-steady state kinetics.

Declaration of Competing Interest

The authors declare that they have no known competing financial interests or personal relationships that could have appeared to influence the work reported in this paper.

Acknowledgements

This paper is part of a special issue to honor the contributions of Isabel Moura and José Moura to the field of metalloproteins. I am grateful to Isabel and José for many years of acting as open-minded, collegial competitors thus sharpening the science of us all.

References

[1] W.R. Hagen, A.J. Pierik, C. Veeger, Novel electron paramagnetic resonance signals from an Fe/S protein containing six iron atoms, J. Chem. Soc., Faraday Trans. 85 (12) (1989) 4083, https://doi.org/10.1039/f19898504083.
[2] A.F. Arendsen, J. Hadden, G. Card, A.S. McAlpine, S. Bailey, V. Zaitsev, E.H.M. Duke, P.F. Lindley, M. Kröckel, A.X. Trautwein, M.C. Feiters, J.M. Charnock, C.D. Garner, S.J. Marritt, A.J. Thomson, I.M. Kooter, M.K. Johnson, W.A.M. van den Berg, W.M.A.M. van Dongen, W.R. Hagen, The "prismane" protein resolved: X-ray structure at 1.7 Å and multiple spectroscopy of two novel 4Fe clusters, J. Biol. Inorg. Chem. 3 (1998) 81–95.
[3] J. Wang, C.E. Vine, B.K. Balasiny, J. Rizk, C.L. Bradley, M. Tinajero-Trejo, R.K. Poole, L.L. Bergaust, L.R. Bakken, J.A. Cole, The roles of the hybrid cluster protein, Hcp, and its reductase, Hcr, in high affinity nitric oxide reduction that protects anaerobic cultures of *Escherichia coli* against nitrosative stress, Mol. Microbiol. 100 (5) (2016) 877–892.
[4] D. Seth, D.T. Hess, A. Hausladen, L. Wang, Y.-J. Wang, J.S. Stamler, A multiplex enzymatic machinery for cellular protein S-nitrosylation, Mol. Cell 69 (3) (2018) 451–464.e6.
[5] D. Aragão, S. Macedo, E.P. Mitchell, C.V. Romão, M.Y. Liu, C. Frazão, L.M. Saraiva, A.V. Xavier, J. LeGall, W.M.A.M. van Dongen, W.R. Hagen, M. Teixeira, M.A. Carrondo, P. Lindley, Reduced hybrid cluster proteins (HCP) from *Desulfovibrio desulfuricans* ATCC 27774 and *Desulfovibrio vulgaris* (Hildenborough): X-ray structures at high resolution using synchrotron radiation, J. Biol. Inorg. Chem. 8 (2003) 540–548.
[6] E.C. Wittenborn, M. Merrouch, C. Ueda, L. Fradale, C. Léger, V. Fourmond, M.-E. Pandelia, S. Dementin, C.L. Drennan, Redox-dependent rearrangements of the NiFeS cluster of carbon monoxide dehydrogenase, eLIFE 7 (2018).
[7] A.F. Arendsen, P.F. Lindley, The search for a "prismane" Fe-S protein, Adv. Inorg. Chem. 47 (1999) 219–249.
[8] M.T. Wolfe, J. Heo, J.S. Garavelli, P.W. Ludden, Hydroxylamine reductase activity of the hybrid cluster protein from *Escherichia coli*, J. Bacteriol 184 (21) (2002) 5898–5902.
[9] C.C. Almeida, C.V. Romão, P.F. Lindley, M. Teixeira, L.M. Saraiva, The role of the hybrid cluster protein in oxidative stress defense, J. Biol. Chem. 281 (43) (2006) 32445–32450.
[10] M.G. Kanatzidis, W.R. Hagen, W.R. Dunham, R.K. Lester, D. Coucouvanis, Metastable Fe/S clusters. The synthesis, electronic structure, and transformations of the $[Fe_6S_6(L)_6]^{3-}$ clusters (L = Cl^-, Br^-, I^-, RS^-, RO^-) and the structure of $[(C_2H_5)_4N]_3[Fe_6S_6Cl_6]$, J. Am. Chem. Soc. 107 (1985) 953-961.
[11] A.J. Pierik, R.B.G. Wolbert, P.H.A. Mutsaers, W.R. Hagen, C. Veeger, Purification and biochemical characterization of a putative [6Fe-6S] prismane-cluster-containing protein from *Desulfovibrio vulgaris* (Hildenborough), Eur. J. Biochem. 206 (1992) 679–704.
[12] I. Moura, P. Tavares, J.J. Moura, N. Ravi, B.H. Huynh, M.Y. Liu, J. LeGall, Direct spectroscopic evidence for the presence of a 6Fe cluster in an iron-sulfur protein isolated from *Desulfovibrio desulfuricans* (ATCC 27774), J. Biol. Chem. 267 (7) (1992) 4489–4496.
[13] W.A.M. van den Berg, A.A.M. Stevens, M.F.J.M. Verhagen, W.M.A.M. van Dongen, W.R. Hagen, Overproduction of the prismane protein from *Desulfovibrio desulfuricans* ATCC 27774 in *Desulfovibrio vulgaris* (Hildenborough) and EPR spectroscopy of the [6Fe-6S] cluster in different redox states, Biochim. Biophys. Acta 1206 (2) (1994) 240–246.
[14] W.R. Hagen, W.A.M. van den Berg, W.M.A.M. van Dongen, E.J. Reijerse, P.J.M. van Kan, EPR spectroscopy of biological iron-sulfur clusters with spin-admixed S = 3/2 ground states, J. Chem. Soc., Faraday Trans. 94 (1998) 2969–2973.
[15] A.J. Pierik, W.R. Hagen, W.R. Dunham, R.H. Sands, Multi-frequency EPR and high-resolution Mössbauer spectroscopy of a putative [6Fe-6S] prismane-cluster-containing protein from *Desulfovibrio vulgaris* (Hildenborough), Eur. J. Biochem. 206 (1992) 705–719.
[16] P. Tavares, A.S. Pereira, C. Krebs, N. Ravi, J.J.G. Moura, I. Moura, B.H. Huynh, Spectroscopic characterization of a novel tetranuclear Fe cluster in an iron-sulfur protein isolated from *Desulfovibrio desulfuricans*, Biochemistry 37 (9) (1998) 2830–2842.
[17] A.S. Pereira, P. Tavares, C. Krebs, B.H. Huynh, F. Rusnak, I. Moura, J.J.G. Moura, Biochemical and spectroscopic characterization of overexpressed fuscoredoxin from *Escherichia coli*, Biochem. Biophys. Res. Commun. 260 (1) (1999) 209–215.
[18] W.A.M. van den Berg, W.R. Hagen, W.M.A.M. van Dongen, The hybrid-cluster protein ('prismane protein') from *Escherichia coli*; characterization of the hybrid-cluster protein, redox properties of the [2Fe-2S] and [4Fe-2S-2O] clusters and identification of an associated NADH oxidoreductase containing FAD and [2Fe-2S], Eur. J. Biochem. 267 (3) (2000) 666–676.
[19] W.R. Hagen, A. van Berkel-Arts, K.M. Krüse-Wolters, G. Voordouw, C. Veeger, The iron-sulfur composition of the active site of hydrogenase from Desulfovibrio vulgaris (Hildenborough) deduced from its subunit structure and total iron-sulfur content, FEBS Lett. 203 (1986) 59–63.
[20] W.R. Hagen, H. Wassink, R.R. Eady, B.E. Smith, H. Haaker, Quantitative EPR of an S = 7/2 system in thionine-oxidized MoFe proteins of nitrogenase. A redefinition of the P-cluster concept, Eur. J. Biochem. 169 (3) (1987) 457–465.
[21] M.S.M. Jetten, A.J. Pierik, W.R. Hagen, EPR characterization of a high-spin system in carbon monoxide dehydrogenase from *Methanothrix soehngenii*, Eur. J. Biochem. 202 (3) (1991) 1291–1297.
[22] R.L.L. Eggen, R. van Kranenburg, A.J.M. Vriesema, A.C.M. Geerling, M.F.J.M. Verhagen, W.R. Hagen, W.M. de Vos, Carbon monoxide dehydrogenase from *Methanosarcina frisia* Gö1. Characterization of the enzyme and the regulated expression of two operon-like *cdh* gene clusters, J. Biol. Chem. 271 (1996) 14256–14263.
[23] A.F. Arendsen, Superclusters. A search for novel structures and functions of biological iron-sulfur clusters, PhD thesis 1996, Wageningen University, edepot.wur.nl/200250.
[24] D.C. Rees, Great metalloclusters in enzymology, Annu. Rev. Biochem. 71 (1) (2002) 221–246.
[25] O. Einsle, D.C. Rees, Structural enzymology of nitrogenase enzymes, Chem. Rev. 120 (12) (2020) 4969–5004.
[26] H.L. Rutledge, F.A. Tezcan, Electron transfer in nitrogenase, Chem. Rev. 120 (12) (2020) 5158–5193.
[27] H. Land, M. Senger, G. Berggren, S.T. Stripp, Current state of [FeFe]-hydrogenase research: biodiversity and spectroscopic investigations, ACS Catal. 10 (2020) 7069–7086.
[28] S.R. Pauleta, M.S.P. Carepo, I. Moura, Source ad reduction of nitrous oxide, Coord. Chem. Rev. 387 (2019) 436–449.
[29] S.C. Rathnayaka, N.P. Mankad, Coordination chemistry of the Cu_Z site in nitrous oxide reductase and its synthetic mimics, Coord. Chem. Rev. 429 (2021) 213718.
[30] H. Tai, S. Hirota, Mechanism and application of the catalytic reaction of [NiFe] hydrogenase: recent developments, ChemBioChem 21 (2020) 1573–1581.
[31] S. Frielingsdorf, J. Fritsch, A. Schmidt, M. Hammer, J. Löwenstein, E. Siebert, V. Pelmenschikov, T. Jaenicke, J. Kalms, Y. Rippers, F. Lendzian, I. Zebger, C. Teutloff, M. Kaupp, R. Bittl, P. Hildebrandt, B. Friedrich, O. Lenz, P. Scheerer, Reversible [4Fe-3S] cluster morphing in an O_2-tolerant [NiFe] hydrogenase, Nat. Chem. Biol. 10 (5) (2014) 378–385.
[32] P.M. Matias, C.M. Soares, L.M. Saraiva, R. Coelho, J. Morais, J. Le Gall, M.A. Carrondo, [NiFe] hydrogenase from *Desulfovibrio desulfuricans* ATCC 27774: gene sequencing, three-dimensional structure determination and refinement at 1.8 Å and modelling studies of its interaction with the tetrahaem cytochrome c_3, J. Biol. Inorg. Chem. 6 (2001) 63–81.
[33] M.C. Marques, R. Coelho, A.L. De Lacey, I.A.C. Pereira, P.M. Matias, The three-dimensional structure of [NiFeSe] hydrogenase from *Desulfovibrio vulgaris* Hildenborough: a hydrogenase without a bridging ligand in the active site in its oxidized, "as isolated" state, J. Mo. Biol. 396 (2010) 893–907.

[34] M.C. Marques, R. Coelho, I.A.C. Pereira, P.M. Matias, Redox state dependent changes in the crystal structure of [NiFeSe] hydrogenase from *Desulfovibrio vulgaris* Hildenborough, Int. J. Hydrogen Energy 38 (2013) 8664–8682.

[35] M.C. Marques, C. Tapia, O. Gutiérrez-Sanz, A.R. Ramos, K.L. Keller, J.D. Wall, A. L. De Lacey, P.M. Matias, I.A.C. Pereira, The direct role of selenocysteine in [NiFeSe] hydrogenase maturation and catalysis, Nature, Chem. Biol. 13 (5) (2017) 544–550.

[36] P. Zanello, Structure and electrochemistry of proteins harboring iron-sulfur clusters of different nuclearities, Part IV. Canonical, non-canonical and hybrid iron-sulfur proteins, J. Struct. Biol. 205 (2) (2019) 103–120.

[37] S. Macedo, E.P. Mitchell, C.V. Romão, S.J. Cooper, R. Coelho, M.Y. Liu, A.V. Xavier, J. LeGall, S. Bailey, C.D. Garner, W.R. Hagen, M. Tiexeira, M.A. Carrondo, P. Lindley, Hybrid cluster proteins (HCPs) from *Desulfovibrio desulfuricans* ATCC 27774 and *Desulfovibrio vulgaris* (Hildenborough): X-ray structures at 1.25 Å resolution using synchrotron radiation, J. Bio Inorg. Chem. 7 (2002) 514–525.

[38] D. Aragão, E.P. Mitchell, C.F. Frazão, M.A. Carrondo, P.F. Lindley, Structural and functional relationships in the hybrid cluster protein family: structure of the anaerobically purified hybrid cluster protein from *Desulfovibrio vulgaris* at 1.35 Å resolution, Acta Crystallograph D 64 (2008) 665–674.

[39] S. Macedo, D. Aragão, E.P. Mitchell, P. Lindley, Structure of the hybrid cluster protein (HCP) from *Desulfovibrio desulfuricans* ATCC 27774 containing molecules in the oxidized and reduced states, Acta Crystallograph. D 59 (12) (2003) 2065–2071.

[40] J.P.W.G. Stokkermans, P.H.J. Houba, A.J. Pierik, W.R. Hagen, W.M.A.M. Dongen, C. Veeger, Overproduction of prismane protein in *Desulfovibrio vulgaris* (Hildenborough); evidence for a second S = 1/2-spin system in the one-electron reduced state, Eur. J. Biochem. 210 (3) (1992) 983–988.

[41] P. Cabello, C. Pino, M.F. Olmo-Mira, F. Castillo, M.D. Roldán, C. Moreno-Vivián, Hydroxylamine assimilation by *Rhodobacter capsulatus* E1F1; requirement of the *hcp* gene (hybrid cluster protein) located in the nitrate assimilation *nas* region for hydroxylamine reduction, J. Biol. Chem. 279 (44) (2004) 45485–45494.

[42] W.R. Hagen, EPR spectroscopy of putative enzyme intermediates on the NO reductase and auto-nitrosylation reaction of Desulfovibrio vulgaris hybrid cluster protein, FEBS Lett. 593 (2019) 3075–3083.

[43] S.J. Marritt, J.A. Farrar, J.L.J. Breton, W.R. Hagen, A.J. Thomson, Characterization of the prismane protein from *Desulfovibrio vulgaris* (Hildenborough) by low-temperature magnetic circular dichroic spectroscopy, Eur. J. Biochem. 232 (2) (1995) 501–505.

[44] M. Kröckel, A.X. Trautwein, A.F. Arendsen, W.R. Hagen, The prismane protein resolved; Mössbauer investigations of a 4Fe cluster with an unusual mixture of bridging ligands and metal coordinations, Eur. J. Biochem. 251 (1998) 454–461.

[45] M. Kröckel, A.X. Trautwein, H. Winkler, A.F. Arendsen, W.R. Hagen, Discovery of novel iron clusters in proteins by Mössbauer spectroscopy, Hyperfine Interact. 113 (1998) 3–14.

[46] R. Lis, S. Brugière, C. Baffert, Y. Couté, W. Nitschke, A. Atteia, Hybrid cluster proteins in a photosynthetic microalga, FEBS J. 287 (4) (2020) 721–735.

[47] M.J. Carney, G.C. Papaefthymiou, R.B. Frankel, R.H. Holm, Alternative spin states in synthetic analogues of biological [4Fe-4S]$^{+}$ clusters: further cases of variable ground states and the structure of $(Et_4N)_3[Fe_4S_4(S\text{-}o\text{-}C_6H_4StBu)_4]$, containing a reduced cluster with compressed tetragonal distortion, Inorg. Chem. 28 (1989) 1497–1503.

[48] H. Rupp, K.K. Rao, D.O. Hall, R. Cammack, Electron spin relaxation of iron-sulphur proteins studied by microwave power saturation, Biochim. Biophys. Acta 537 (2) (1978) 255–269.

[49] B. Guigliarelli, P. Bertrand, Application of EPR spectroscopy to the structural and functional study of iron-sulfur proteins, Adv. Inorg. Chem. 47 (1999) 421–497.

[50] T. Fujishiro, M. Ooi, K. Takaoka, Crystal structure of *Escherichia coli* class II hybrid cluster protein, HCP, reveals a [4Fe-4S] cluster at the N-terminal protrusion, FEBS J. 288 (23) (2021) 6752–6768.

[51] M.L. Overeijnder, W.R. Hagen, P.-L. Hagedoorn, A thermostable hybrid cluster protein from Pyrococcus furiosus: effect of the loss of a three helix bundle subdomain, J. Biol. Inorg. Chem. 14 (2009) 703–710.

[52] K.-L. Han, T.-S. Yong, J.S. Ryu, U.W. Hwang, S.J. Park, Identification of the hybrid cluster protein, HCP, from amitochndriate eukaryotes and its phylogenetic implications, J. Microbiol. Biotechnol. 14 (2004) 134–139.

[53] J.P.W.G. Stokkermans, A.J. Pierik, R.B.G. Wolbert, W.R. Hagen, W.M.A.M. Dongen, C. Veeger, The primary structure of a protein containing a putative [6Fe-6S] prismane cluster from *Desulfovibrio vulgaris* (Hildenborough), Eur. J. Biochem. 208 (2) (1992) 435–442.

[54] M. Inoue, I. Nakamoto, K. Omae, T. Oguro, H. Ogata, T. Yoshida, Y. Sako, Structural and phylogenetic diversity of anaerobic carbon-monoxide dehydrogenases, Frontiers Microbiol. 9 (2019) fmicb2018.03353.

[55] L.C. Valk, M. Diender, G.R. Stouten, J.F. Petersen, P.H. Nielsen, M.S. Dueholm, J. T. Pronk, M.C.M. van Loosdrecht, "Candidatus Galacturonibacter souhngenii" shows acetogenic catabolism of galacturonic acid but lacks a canonical carbon monoxide dehydrogenase/acetyl-CoA synthase complex, Frontiers Microbiol. 11 (2020) micb.2020.00063.

[56] J.O. Andersson, Å.M. Sjögren, L.A.M. Davis, T.M. Embley, A.J. Roger, Phylogenetic analyses of diplomonad genes reveal frequent lateral gene transfers affecting eukaryotes, Curr. Biol. 13 (2) (2003) 94–104.

[57] J.O. Andersson, R.P. Hirt, P.G. Foster, A.J. Roger, Evolution of four gene families with patchy phylogenetic distributions: influx of genes into protest genomes, BMC Evolution. Biol. 6 (2006) DOI: 0.1186/1471-2148-6-27.

[58] D.A. Rodionov, I. Dubchak, A. Arkin, E. Alm, M.S. Gelfand, Reconstruction of regulatory and metabolic pathways in metal-reducing δ-proteobacteria, Genome Biol. 5 (2004) R90.

[59] D.A. Rodionov, I.L. Dubchak, A.P. Arkin, E.J. Alm, M.S. Gelfand, Dissimilatory metabolism of nitrogen oxides in bacteria: comparative reconstruction of transcriptional networks, PLoS Comput. Biol. 1 (2005) 415–431.

[60] I.T. Cadby, S.J.W. Busby, J.A. Cole, An HcpR homologue from *Desulfovibrio desulfuricans* and its possible role in nitrate reduction and nitrosative stress, Biochem. Soc. Trans. 39 (2011) 224–229.

[61] A. Zhou, Y.I. Chen, G.M. Zane, Z. He, C.L. Hemme, M.P. Joachimiak, J.K. Baumohl, Q. He, M.W. Fields, A.P. Arkin, J.D. Wall, T.C. Hazen, J. Zhou, Functional characterization of Crp/Fnr-type global transcriptional regulators in *Desulfovibrio vulgaris* Hildenborough, Appl. Environ. Microbiol. 78 (4) (2012) 1168–1177.

[62] S.M. da Silva, C. Amaral, S.S. Neves, C. Santos, C. Pimentel, C. Rodrigues-Pousada, An HcpR paralog of Desulfovibrio gigas provides protection against nitrosative stress, FEBS Open Bio 5 (2015) 594–604.

[63] I.T. Cadby, S.A. Ibrahim, M. Faulkner, D.J. Lee, D. Browning, S.J. Busby, A.L. Lovering, M.R. Stapleton, J. Green, J.A. Cole, Regulation, sensory domains and roles of two Desulfovibrio desulfuricans ATCC27774 Crp family transcription factors, HcpR1 and HcpR2, in response to nitrosative stress, Mol. Microbiol. 102 (6) (2016) 1120–1137.

[64] I.T. Cadby, M. Faulkner, J. Cheneby, J. Long, J. van Helden, A. Dolla, J.A. Cole, Coordinated response of the *Desulfovibrio desulfuricans* 27774 transcriptome to nitrate, nitrite and nitric oxide, Sci. Rep. 7 (2017) 16228.

[65] M.-C. Boutrin, C. Wang, W. Arundi, X. Li, H.M. Fletcher, Nitric oxide stree resistance in *Porphyromonas gingivalis* is mediated by a putative hydroxylamine reductase, J. Bacteriol. 194 (2012) 1582–1592.

[66] J.P. Lewis, S.S. Yanamandra, C. Anaya-Bergman, J.B. Bliska, HcpR of *Porphyromonas gingivalis* is required for growth under nitrosative stress and survival within host cells, Infect. Immunol. 80 (9) (2012) 3319–3331.

[67] B.R. Belvin, Q. Gui, J.A. Hutcherson, J.P. Lewis, M. Whiteley, The Porphyromonas gingivalis hybrid cluster protein Hcp is required for growth with nitrite and survival with host cells, Infect. Immunol. 87 (4) (2019), https://doi.org/10.1128/IAI.00572-18.

[68] K.R. Jones, B.R. Belvin, F.L. Macrina, J.P. Lewis, Sequence and characterization of shuttle vectors for molecular cloning in *Porphyromonas*, *Bacteroides* and related bacteria, Mol. Oral Microbiol. 35 (4) (2020) 181–191.

[69] D.L. Chismon, D.F. Browning, G.K. Farrant, S.J.W. Busby, Unusual organization, complexity and redundancy at the *Escherichia coli* hcp-hcr operon promotor, Biochem. J. 430 (2010) 61–68.

[70] N.A. Filenko, D.E. Browning, J.A. Cole, Transcriptional regulation of a hybrid cluster (prismane) protein, Biochem. Soc. Trans. 33 (2005) 195–197.

[71] N. Filenko, S. Spiro, D.F. Browning, D. Squire, T.W. Overton, J. Cole, C. Constantinidou, The NsrR regulon of *Escherichia coli* K-12 includes genes encoding the hybrid cluster protein and the periplasmic, respiratory nitrite reductase, J. Bacteriol. 189 (12) (2007) 4410–4417.

[72] J.D. Partridge, D.M. Bodenmiller, M.S. Humphrys, S. Spiro, NsrR targets in *Escherichia coli* genome: new insights into DNA sequence requirements for binding and a role for NsrR in the regulation of motility, Mol. Microbiol. 73 (2009) 680–694.

[73] S. Spiro, Regulators of bacterial responses to nitric oxide, FEMS Microbiol. Rev. 31 (2) (2007) 193–211.

[74] J. Heo, M.T. Wolfe, C.R. Staples, P.W. Ludden, Converting the NiFeS carbon monoxide dehydrogenase to a hydrogenase and a hydroxylamine reductase, J. Bacteriol. 184 (21) (2002) 5894–5897.

[75] J. Mager, A TPNH-linked sulphite reductase and its relation to hydroxylamine reductase in enterobacteriaceae, Biochim. Biophys. Acta 41 (1960) 553–555.

[76] L.M. Siegel, P.S. Davis, H. Kamin, Reduced nicotinamide adenine dinucleotide phosphate-sulfite reductase of enterobacteria III. The *Escherichia coli* hemoflavoprotein: catalytic parameters and the sequence of electron flow, J. Biol. Chem. 249 (1974) 1572–1586.

[77] J. Ostrowski, M.J. Barber, D.C. Rueger, B.E. Miller, L.M. Siegel, N.M. Kredich, Characterization of the flavoprotein moieties of NADPH-sulfite reductase from *Salmonella typhimurium* and *Escherichia coli*, J. Biol. Chem. 264 (27) (1989) 15796–15808.

[78] K. Kobayashi, Y. Seki, M. Isomoto, Biochemical studies on sulfate-reducing bacteria XIII. Sulfite reductase from *Desulfovibrio vulgaris* – mechanism of trithionate, thiosulfate, and sulphide formation and enzymatic properties, J. Biochem. 75 (1974) 519–529.

[79] M. Tanno-Nakanishi, Y. Kikuchi, E. Kokubu, S. Yamada, K.I. Ishihara, *Treponema denticola* transcriptional profiles in serum-restricted conditions, FEMS Microbiol. Lett. 365 (2018) fny171.

[80] J. Przybyla-Toscano, J. Couturier, C. Remacle, N. Rouhier, Occurrence, evolution and specificities of iron-sulfur proteins and maturation factors in chloroplasts from algae, Int. J. Mol. Sci. 22 (2021) 3175.

[81] A.L. Brioukhanov, M.-C. Durand, A. Dolla, C. Aubert, Response of *Desulfovibrio vulgaris* Hildenborough to hydrogen peroxide: enzymatic and transcriptional analyses, FEMS Microbiol. Lett. 310 (2010) 175–181.

[82] E.D. Coulter, D.M. Kurtz Jr, A role for rubredoxin in oxidative stress protection in *Desulfovibrio vulgaris*: catalytic electron transfer to rubrerythin and two-iron superoxide reductase, Arch. Biochem. Biophys. 394 (2001) 76–86.

[83] N.A. Botwright, A.R. Mohamed, J. Slinger, P.C. Lima, J.W. Wynne, Host-parasite interaction of atlantic salmon (Salmo salar) and the ectoparasite *Neoparamoeba perurans* in amoebic gill disease, Frontiers Immunol. 12 (2021) 672700.
[84] B. Balasiny, M.D. Rolfe, C. Vine, C. Bradley, J. Green, J. Cole, Release of nitric oxide by the *Escherichia coli* YtfE (RIC) protein and its reduction by the hybrid cluster protein in an integrated pathway to minimize cytoplasmic nitrosative stress, Microbiology 164 (2018) 563–575.
[85] P. Girsch, S. de Vries, Purification and initial kinetic and spectroscopic characterization of NO reductase from *Paracoccus denitrificans*, Biochim. Biophys. Acta 1318 (1-2) (1997) 202–216.
[86] S. Bulot, S. Audebert, L. Pieulle, F. Seduk, E. Baudelet, L. Espinosa, M.-C. Pizay, L. Camoin, A. Magalon, M.W. Ribbe, Clustering as a means to control nitrate respiration efficiency and toxicity in *Escherichia coli*, Mol. Biol. Physiol. 10 (5) (2019), https://doi.org/10.1128/mBio.01832-19.
[87] S.-H. Gao, J.Y. Ho, L. Fan, A. Nouwens, R.D. Hoelzle, B. Schulz, J. Guo, J. Zhou, Z. Yuan, P.I. Bond, A comparative proteomics analysis of *Desulfovibrio vulgaris* Hildenborough in response to the antimicrobial agent free nitrous acid, Sci. Total Environm. 672 (2019) 625–633.
[88] Z. Yu, M. Pesesky, L. Zhang, J. Huang, M. Winkler, L. Chistoserdova, A. Shade, A complex interplay between nitric oxide, quorum sensing, and the unique secondary metabolite tundrenone constitutes the hypoxia response in *Methylobacter*, Mol. Biol. Physiol. 5 (1) (2020), https://doi.org/10.1128/mSystems.00770-19.
[89] D. Seth, A. Hausladen, Y.-J. Wang, J.S. Stamler, Endogenous protein S-nitrosylation in *E. coli*: regulation by OxyR, Science 336 (2012) 470–473.
[90] J.A. Cole, Anaerobic bacterial response to nitric oxide stress: widespread misconceptions and physiologically relevant responses, Mol. Microbiol. (early view) 116 (1) (2021) 29–40, https://doi.org/10.1111/mmi.14713.
[91] R.R. Dyer, K.I. Ford, R.A.S. Robinson, The roles of S-nitrosylation and S-glutathionylation in Alzheimer's disease, Methods Enzymol 626 (2019) 499–538.
[92] A.J. Hobbach, E.I. Closs, Human cationic amino acid transporters are not affected by direct nitros(yl)ation, Amino Acids 52 (3) (2020) 499–503.
[93] N. Marozkina, B. Gaston, An update on thiol signalling: S-nitrosothiols, hydrogen sulphide and a putative role for thionitrous acid, Antioxidants 9 (2020) 225.
[94] C. Montagna, C. Cirotti, S. Rizza, G. Filomeni, When S-nitrosylation gets to mitochondria: from signalling to age-related diseases, Antioxid. Redox Signal. 32 (2020) ars.2019.7872.
[95] D. Seth, A. Hausladen, J.S. Stamler, Anaerobic transcription by OxyR: a novel paradigm for nitrosative stress, Antioxid. Redox Signal. 32 (2020) ars.2019.7921.
[96] W.-H. Cheng, K.-Y. Huang, S.-C. Ong, F.-M. Ku, P.-J. Huang, C.-C. Lee, Y.-M. Yeh, R. Lin, C.-H. Chiu, P. Tang, Protein cysteine S-nitrosylation provides reducing powerby enhancing lactate dehydrogenase activity in *Trichomonas vaginalis* under iron deficiency, Parasites Vectors 13 (2020) 477.
[97] C.M. Bellido-Pedraza, V. Calatrava, E. Sanz-Luque, M. Tejada-Jiménez, Á. Llames, M. Plouviez, B. Guieysse, E. Fernández, A. Galván, *Chlamydomonas reinhardtii*, an algal model in the nitrogen cycle, Plants 9 (2020) 903.
[98] O. Ulloa, C. Henríquez-Castillo, S. Ramirez-Flandres, A.M. Plominsky, A.A. Murillo, C. Morgan-Lang, S.J. Hallam, R. Stepanauskas, The cyanobacterium *Prochlorococcus* has divergent light-harvesting antennae and may have evolved in a low-oxygen ocean, Proc. Natl. Acad. Sci. 118 (2021) e2025638118.
[99] N. Barraud, S. Létoffé, C. Beloin, J. Vinh, G. Chiappetta, J.-M. Chigo, Lifestyle-specific S-nitrosylation of protein cysteine thiols regulates *Escherichia coli* biofilm formation and resistance tooxidative stress, Biofilms Microbiomes 7 (2021) 34.
[100] A. Arendsen, Y. Bulsink, W. Hagen, J. Hadden, G. Card, A.S. McAlpine, S. Bailey, V. Zaitsev, P. Lindley, Crystallization and preliminary X-ray crystallographic analysis of the putative [6Fe-6S] prismane protein from *Desulfovibrio vulgaris* (Hildenborough), Acta. Cryst. D 52 (6) (1996) 1211–1213.
[101] S.J. Cooper, C.D. Garner, W.R. Hagen, P.F. Lindley, S. Bailey, Hybrid-cluster protein (HCP) from *Desulfovibrio vulgaris* (Hildenborough) at 1.6 Å resolution, Biochemistry 39 (49) (2000) 15044–15054.
[102] M.L. de Vocht, I.M. Kooter, Y.B.M. Bulsink, W.R. Hagen, M.K. Johnson, Resonance Raman evidence for non-heme Fe-O species in the [6Fe-6S]-containing iron-sulfur protein from sulfate-reducing bacteria, J. Am. Chem. Soc. 118 (1996) 2766–2767.
[103] H. Dobbek, V. Svetlitchnyi, L. Gremer, R. Huber, O. Meyer, Crystal structure of a carbon monoxide dehydrogenase reveals a [Ni-4Fe-5S] cluster, Science 293 (5533) (2001) 1281–1285.
[104] C.L. Drennan, J. Heo, M.D. Sintchak, E. Schreiter, P.W. Ludden, Life on carbon monoxide: X-ray structure of Rhodospirillum rubrum Ni-Fe-S carbon monoxide dehydrogenase, Proc. Natl. Acad. Sci. USA 98 (2001) 11873–11878.
[105] M.E. Anderson, P.A. Lindahl, Spectroscopic states of the CO oxidation/CO_2 reduction active site of carbon monoxide dehydrogenase and mechanistic implications, Biochemistry 35 (25) (1996) 8371–8380.